SAN FRANCISCO ESTUARY & WATERSHED SCIENCE
Sponsored by the Delta Science Program and UC Davis Institute for the Environment

RESEARCH

What Controls Suspended-Sediment Concentration and Export in Flooded Agricultural Tracts in the Sacramento–San Joaquin Delta?

Jessica R. Lacy*[1], Evan T. Dailey[1], Tara L. Morgan–King[2]

ABSTRACT

We investigated wind-wave and suspended-sediment dynamics in Little Holland Tract and Liberty Island, two subsided former agricultural tracts in the Cache Slough complex in the northern Sacramento–San Joaquin Delta which were restored to tidal shallows to improve habitat. Turbidity, and thus suspended-sediment concentration (SSC), is important to habitat quality because some species of native fishes, including the Delta Smelt, are found preferentially in more turbid waters. Data from October 2015 to August 2016 show that average SSC was greater within Little Holland Tract than in the primary breach that connects the basin to surrounding channels: approximately twice as great at a shallower station farther from the breach and 15% greater at a deeper station closer to the breach. Suspended-sediment concentration within Little Holland Tract was directly related to wave shear stress and inversely related to water depth, based on linear regression. We used measurements of suspended-sediment flux (SSF) through the largest levee breaches to assess whether the enhanced SSC within Little Holland Tract is exported to surrounding waters, thus potentially increasing turbidity over a wider region. Cumulatively, sediment is exported through the Little Holland Tract breaches in winter and imported in summer, consistent with regional patterns in sediment flux, indicating that wind-wave resuspension within the basin does not control sediment flux from Little Holland Tract on seasonal time-scales. Some sediment was exported during wind-wave events, and results show that sediment export is greater when primary breaches are located downwind of the basin rather than upwind.

KEY WORDS

sediment transport, suspended-sediment concentration, sediment particle size, shallow water habitat, wind waves, wind-wave resuspension, Little Holland Tract, Liberty Island, Cache Slough complex, Sacramento–San Joaquin Delta

SFEWS Volume 21 | Issue 1 | Article 4

https://doi.org/10.15447/sfews.2023v21iss1art4

* Corresponding author: jlacy@usgs.gov

1 US Geological Survey
Pacific Coastal and Marine Science Center
Santa Cruz, CA 95060 USA

2 US Geological Survey
California Water Science Center
Sacramento CA, 95826 USA

INTRODUCTION

The Sacramento–San Joaquin Delta (Delta) is an extensive tidal, freshwater region at the landward boundary of the San Francisco Estuary which has been highly modified by human activities, including large-scale habitat restoration in recent decades. The Delta ecosystem has deteriorated as a result of loss of habitat complexity, water diversion, contaminants, and invasive species, and these effects are now exacerbated by a changing climate and rising sea levels (Luoma et al. 2015). Native fish populations, including the Delta Smelt (*Hypomesus transpacificus)* have been particularly affected (Nichols et al. 1986; Sommer et al. 2007). The endemic Delta Smelt population has declined enough to warrant their listing as endangered and threatened by the California and federal Endangered Species Acts, respectively (Moyle et al. 1992; Hasenbein et al. 2013; CNDDB 2023).

The decline of Delta Smelt has been correlated with a reduction in turbidity in Delta waters, among other factors, such as competition from introduced species (Moyle et al. 1992; Feyrer et al. 2007; Sommer and Mejia 2013). High turbidity benefits Delta Smelt by providing background contrast for prey recognition and camouflage from predation (Bennett and Moyle 1996; Sommer and Mejia 2013; Bever et al. 2016). Turbidity, which in the Delta is predominantly produced by sediment in suspension, declined by about 50% between 1957 and 2001 (Schoellhamer and Wright 2003; Wright and Schoellhamer 2004; Hestir et al. 2016; Work et al. 2021).

In recent decades, both the state of California and the federal government have invested in large-scale habitat restoration in the Delta. At numerous sites, including Little Holland Tract and Liberty Island, levees surrounding subsided agricultural tracts were breached (either intentionally or not), creating shallow tidal basins. The functioning of these restored shallows has been a topic of debate and research. An interdisciplinary study in Franks Tract and Mildred Island in the central Delta addressed phytoplankton dynamics, hydrodynamics, and benthic grazing (Lucas et al. 2002, 2006; Lopez et al. 2006). Jones at al. (2008) studied wind-wave dynamics in Franks Tract, and Lehman et al. (2010) reported seasonal variation in the direction of flux of organic and inorganic substances into and out of Liberty Island. The suitability of shallows such as Liberty Island for Delta Smelt is discussed by Sommer and Mejia (2013). Our work was part of an interdisciplinary study that investigated physical and biological factors contributing to habitat quality in flooded shallows and other Delta environments conducted by the US Geological Survey with funding from the Bureau of Reclamation.

This paper addresses wind-wave and sediment dynamics within Little Holland Tract and Liberty Island and the potential for elevated turbidity in shallows to influence surrounding waters. Shallow basins are likely to be more turbid than the surrounding channels because their broad expanse allows for the development of wind waves which, in shallow waters, resuspend sediment. These turbid, shallow basins might, in turn, improve habitat over a larger area, but only if the export of suspended sediment is sufficient to increase turbidity in the surrounding waters. Depth, bed sediment properties, wind exposure, basin size, and breach location can influence suspended-sediment concentration (SSC) within basins and suspended-sediment flux (SSF) from basins. Our goals were to determine what controls SSC and sediment export in Little Holland Tract and Liberty Island, to inform future habitat restoration and construction projects. We focus primarily on Little Holland Tract because its levees are more intact than Liberty Island's, so that measurements of water and sediment flux at the major breaches better represent the net flux for the enclosed shallow basin.

We address three questions:

1. What is the range of SSC in Little Holland Tract and Liberty Island, and how does it vary seasonally and with wind and wave conditions?

2. What conditions produce the greatest export of suspended sediment and turbidity from

Little Holland Tract through breaches to surrounding waters?

3. What are the modifiable features of shallow tidal basins that influence the magnitude of sediment export?

METHODS

Study Area

Humans have modified the Delta extensively since the mid 19th century, including diking and filling wetlands for agriculture, dredging channels for navigation, and redirecting and exporting water for agriculture and municipal supply. The result has been a dramatic increase in channelization and a reduction in tidal wetlands. Management of the Delta today is subject to competing demands: protection of the source of fresh water for much of California and protection of a productive yet threatened ecosystem (Luoma et al. 2015).

The Sacramento and San Joaquin rivers supply sediment to the Delta, mostly during high flows, which occur in winter and spring (Conomos et al. 1985; Wright and Schoellhamer 2005). Between 1957 and 2001, sediment delivery to the Delta decreased by about 50% (Wright and Schoellhamer 2004). Causes for the decrease include construction of reservoirs, diking and riverbank armoring, urbanization in the watershed, and long-term effects of the end of hydraulic mining in the Sierra Nevada in the late 19th century. Turbidity in the Delta has declined over the same period, which is attributed to the reduced sediment supply as well as the increasing prevalence of invasive vegetation (Jassby et al. 2002; Hestir et al. 2016; Work et al. 2021).

Little Holland Tract and Liberty Island are located in the North Delta in the Cache Slough complex: a suite of sloughs and channels connected to the Sacramento River. Tides in the Cache Slough complex are mixed semidiurnal, with a mean range of 1.2 m. In dry conditions, tidally averaged SSF in the Cache Slough complex is directed landward (Morgan–King and Schoellhamer 2013). Periods of high winter flows intermittently increase water levels in the Cache Slough complex, reducing tidal influence and producing unidirectional downstream currents. When flows in the Sacramento River are elevated, flow can be routed through the Yolo Bypass to reduce flooding of the Sacramento metropolitan area. The Yolo Bypass terminates at the northern end of the Cache Slough complex, and intermittent flows through the Yolo Bypass deliver water and sediment to the Toe Drain, Little Holland Tract, and Liberty Island.

Little Holland Tract and the adjacent, much larger Liberty Island are connected to the rest of the Cache Slough complex and Sacramento River by a network of channels (Figure 1). The shallow depth and relatively long fetch of Liberty Island and Little Holland Tract along the prevailing southwest wind direction make them susceptible to sediment resuspension by wind waves. Large breaches allow for sediment flux to connecting channels. The subsided Little Holland Tract was flooded in the 1980s when the surrounding levees were breached, but it remains bordered by mostly intact levees. The largest breach is located at the southern end (South Breach), and a second large breach in the northwest (North Breach) connects to the Stairstep Channel (Figure 1). Little Holland Tract is very shallow, and approximately 44% of its area is intertidal: the surface area shrinks from 3.5×10^6 to 1.95×10^6 m^2 between mean higher-high water and mean lower-low water, and the mean depth drops from 1.15 to 0.21 m. The mean low-tide volume is 22% of the mean high-tide volume (3,625,300 m^3) (Snyder, Stevens, et al. 2016).

Winds in the area vary seasonally, with spring and summer winds originating predominantly from the southwest; wind direction in the winter is variable. The orientation of Little Holland Tract offers a relatively large fetch for winds from either the southerly or northerly quadrants.

Data Collection

Inside Little Holland Tract and Liberty Island

We collected *in situ* time-series measurements of hydrodynamics and turbidity from submerged instrument platforms at four stations in Little

https://doi.org/10.15447/sfews.2023v21iss1art4

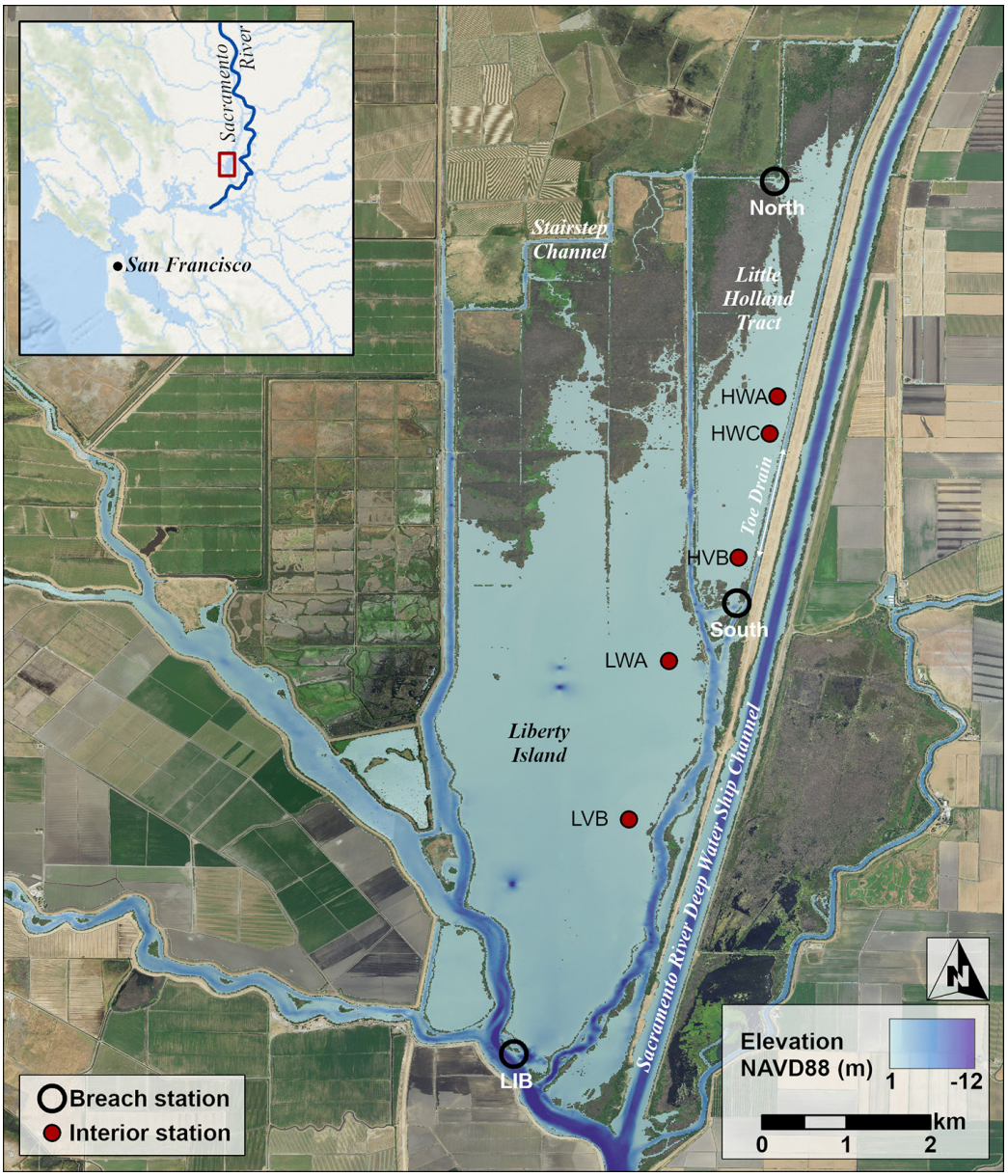

Figure 1 Map of study area in the Sacramento–San Joaquin Delta with station locations. *Sources*: Aerial imagery from US Geological Survey (2014). Bathymetry from Fregoso et al. (2017) displayed where aerial imagery was classified as water.

Holland Tract and Liberty Island (Table 1, Figure 1). At all stations, we measured turbidity, water depth, and wave height and period, which are derived from high-frequency pressure measurements (Table 2). At stations HVB and LVB, we also collected high-frequency bursts of velocity to determine tidal currents, wave direction, and wave velocities. Data were collected over a 27-month period, from August 2015 to October 2017 (Lacy et al. 2016). Little Holland Tract station HWC replaced the nearby station HWA after the initial 4 months of data collection, and we treated HWA and HWC as coincident data, and hereafter refer to the combined data set as HWC.

We measured SSC with optical backscatter sensors (OBS), which measure light scattered by particles suspended in the water column, producing a signal that is linearly related to

Table 1 Average measured water depth, coordinates, and dates of data collection for stations in interior of Little Holland Tract and Liberty Island. *Source*: Lacy et al. 2016, 2019 revision.

Station ID	Depth (m)	Latitude	Longitude	Active dates
HWA	0.57	38°18′44.76″N	121°39′28.41″W	Aug 4, 2015–Dec 7, 2015
HWC	0.58	38°18′30.73″N	121°39′31.46″W	Dec 8, 2015–Oct 3, 2017
HVB	0.65	38°17′42.80″N	121°39′43.38″W	Aug 4, 2015–Oct 3, 2017
LWA	0.67	38°17′2.06″N	121°40′10.30″W	Aug 4, 2015–Oct 3, 2017
LVB	1.37	38°16′2.38″N	121°40′26.99″W	Aug 4, 2015–Aug 9, 2016 Dec 7, 2016–Mar 30, 2017

Table 2 Data types and sampling intervals and frequencies

Station ID	Measured variables	Sampling frequency (Hz)	Burst interval (min)	Burst duration (sec)
HWA, HWC, LWA	Pressure temperature	6	10	170
	SSC	1	5	30
HVB, LVB	Single point velocity	8	20	260
	SSC	8	20	260
	Pressure	16	10	128
HVB	Conductivity temperature pressure		10	10 s avg

SSC (Schoellhamer and Wright 2003). Optical backscatter (OBS) sensors were equipped with wipers that cleaned the sensor every 4 hours and prevented fouling caused by growth directly on the receiver.

Occasionally, vegetation caught on the frames entered into the sampling volume, reducing data quality. Water samples were collected at each station throughout the deployment and analyzed for SSC by filtration in the sediment lab at the US Geological Survey (USGS) Pacific Coastal and Marine Science Center (PCMSC). Calibration coefficients for each OBS were determined from linear regression between SSC and OBS readings and applied to the OBS time-series. The coefficient of determination (R^2) was 0.83 or greater for all sensors (Lacy et al. 2016). The OBS data were post-processed using thresholding to remove spurious values or values above 90% of the instrument's maximum voltage, and points that were removed in this process were filled by linear interpolation if the data gap was 3 hours or shorter. Sporadic periods of clearly erroneous or missing data—as a result of instrument fouling or aerial exposure at extreme low tides—were removed.

Surficial sediments were sampled near the stations inside Little Holland Tract and Liberty Island before the deployment in August 2014, fourteen times during the deployment, and six times in 2018–2019 to characterize the bed sediment particle size distribution (Lacy et al. 2020). Sediments were collected either as grabs with a small Ponar sampler (from August 2015 to April 2016), from which the top 1 to 2 cm were retained, or as short push cores (in 2014 and from June 2016 to August 2019). Cores were obtained by manually pushing a 4.45-cm-diameter plastic tube approximately 10 cm into the bed sediment and were divided into 1-cm vertical sections. For all samples, both the fine fraction (< 63 μm) and sand fraction (63 μm^{-2} mm) were analyzed with a laser diffraction particle analyzer to determine disaggregated grain size distribution at the USGS PCMSC sediment lab.

Samples from August 2014, June 2016, October 2017, and the six sampling dates in 2018–2019 were also analyzed for bulk density, as follows. Push core sections were stored in sealed plastic bags until weighed. Samples were weighed wet, dried to a constant weight at 60 ° C, and weighed again. Dry bulk density was calculated as $BD = (1 - P)\rho_s$, where porosity P is the fraction of water by volume and $\rho_s = 2.65\,g\,cm^{-3}$ is sediment density.

https://doi.org/10.15447/sfews.2023v21iss1art4

Wind and atmospheric pressure data were acquired from hourly records at Travis Air Force Base (Iowa State University 2018), located approximately 23 km west of Little Holland Tract. The topography between Travis and Little Holland Tract is mostly flat, so we assumed winds there represent wind conditions at Little Holland Tract.

Breaches

Water discharge, turbidity, and SSC were measured continuously (15-min intervals) at three levee breaches while we collected data within Little Holland Tract and Liberty Island. In Little Holland Tract, the stations were at the South Breach (USGS site number 11455167, Prospect Slough at Toe Drain) and the North Breach, connecting to the Stairstep Channel (USGS site number 11455143). In Liberty Island, we used data from the long-term monitoring station at the Liberty Island Breach (LIB; USGS site number 11455315, Cache Slough at South Liberty Island near Rio Vista, CA) (Figure 1). USGS reports discharge and SSC representative of the full cross-section at each of these breach locations on the USGS National Water Information System database (*https://waterdata.usgs.gov/ca/nwis*); US Geological Survey, 2020. For all three breaches, positive denotes export (directed out of the basin) for velocity, water flux (also known as discharge), and SSF. USGS methods to compute discharge follow Levesque and Oberg (2012) and Ruhl and Simpson (2005). SSC was computed from measured turbidity using site-specific models between SSC in water samples and turbidity (Morgan–King and Conlen 2021a, 2021b), developed following Rasmussen et al. (2009) and US Geological Survey (2016).

Data Processing

We used data from the period that spanned September 2015 through September 2016 to compare seasonal trends. In late March 2016, elevated Sacramento River flows and a small diversion through the Yolo Bypass produced large downstream water and sediment flux through Little Holland Tract, including several days in which flow was directed downstream throughout the tidal cycle. We defined winter (September 1, 2015 to March 12, 2016) and summer (April 1 to September 1, 2016) to exclude the high-flow period in March, when data quality within Little Holland Tract was low, and discharge estimates were likely not accurate because levees in the region were overtopping. Within these two periods, SSC data are not available for the South Breach for September 12 to November 12, 2015, and discharge data are not available for the North breach for November 1 to December 15, 2015, or for the summer period. Data from 2017 were not used for the seasonal comparisons because of the historic high flows through the Delta during the winter of 2017. High river discharge produces unidirectional flow in the study area, reducing the importance of the tidal exchange processes that are the focus of this paper.

Pressure data from the interior stations were corrected for fluctuations in atmospheric pressure measured at Travis Air Force Base and converted to depth. Wave height and period were calculated from the corrected bursts of pressure data following linear wave theory, which accounts for the depth of the sensor below the water surface. Gaps in the pressure data occurred sporadically, primarily when sensors were out of the water during very low tides. Bed shear stress from waves (τ_w), currents (τ_c), and a combination of waves and currents (τ_{wc}) were calculated for HVB following Grant and Madsen (1979), using measured current velocities and wave statistics. For HWC, we estimated velocity as

$$u_{HWC}\sqrt{h_{HWC}/h_{HVB}},$$

where h is water depth, to use along with measured wave statistics from HWC as inputs in calculating τ_w, τ_c, and τ_{wc}. The estimate for u_{HWC} is derived assuming that the along-channel gradient in water surface elevation and the drag coefficient are equivalent at HVB and HWC, and that the along-channel pressure gradient is balanced by friction, as is typical for open-channel flows.

Water flux at HVB was calculated at 15-minute intervals as the product of measured velocity (neglecting cross-channel variation) and the flooded cross-sectional area of Little Holland

Tract at the latitude of station HVB. The flooded cross-sectional area was determined for each time-step from water depth and a digital elevation model of Little Holland Tract (Snyder, Lacy et al. 2016). Suspended-sediment flux was calculated as SSF = $Q \times$ SSC, where Q is discharge. For both Q and SSF, positive values denote transport in the ebb direction (down-estuary or export from Little Holland Tract or Liberty Island). Suspended-sediment flux was calculated for station HVB inside Little Holland Tract, and for the South, North, and LIB breaches.

Time-series were tidally averaged using a low-pass Butterworth filter (0.033-hour stopband; 0.025-hour passband) to distinguish low-frequency variation from higher-frequency oscillations produced by diurnal and semidiurnal tides and short-term wind events. Tidally averaged SSF was decomposed into a sum of advective and dispersive flux. Advective flux, which constitutes transport by the mean flow, is the product $\langle Q \rangle \times \langle SSC \rangle$, where angle brackets denote tidal average. Dispersive flux, which is produced by tidal-time-scale correlation between tidally varying SSC and discharge, is the product $\langle Q' \times SSC' \rangle$, where prime indicates deviation from the tidally averaged value (Fischer et al. 1979).

To determine the relative importance of factors that influence SSC in Little Holland Tract, we constructed linear regression models with combinations of predictor variables hypothesized to be important to sediment resuspension and compared them using Akaike Information Criterion (AIC) and log evidence ratios (LER) (Burnham and Anderson 2002, 2004). The predictor variables were depth; tide phase (flood or ebb); τ_w, τ_c and τ_{wc}; and the dependent variable was SSC at HVB and HWC. We assumed the predictor variables were independent, although tidal phase, depth, and τ_c may not be fully independent. We tested eleven models, some with single-predictor variables and others with combinations, excluding models that contained multiple dependent shear stress values (τ_{wc} and either τ_c or τ_w). The LER indicates the strength of evidence for rejecting the null hypothesis that a model's fit is equivalent to the "best" model (indicated by the lowest AIC value). Following Kass and Raftery (1995), we classified LER values as minimal ($0 \le LER < 0.5$), substantial ($0.5 \le LER < 1$), strong ($1 \le LER < 2$), or decisive ($LER >= 2$). For this analysis, we used results from April and May 2016.

RESULTS

Bed Sediments

The bed-sediment sampling near stations HWC, HVB, LWA, and LVB encompassed periods of drought (2015) and historic high flows (2017). The top centimeter of core samples tended to exhibit bimodal grain-size distributions, with a peak in the fines fraction (< 63 μm) and in the sand fraction (63 μm–2 mm; Figure 2). While fines constituted more than 50% by weight of most samples, the percent sand was frequently greater than 10%, and varied considerably over time (Figure 3). The temporal variation of the grain-size distributions suggests active sediment deposition and/or erosion during the study period.

To test whether river discharge influenced particle size, we compared the mean percent fines in the surficial sediments during the drought conditions at the beginning of the study (August 2015 to February 2016) to that after the 2017 high flows (May 2017 to August 2019). The mean percent fines increased from 40 ± 7.2% (95% confidence interval) (drought) to 65 ± 1.8% at HWC, from 72 ± 10% (drought) to 89 ± 5.1% at HVB, and from 67 ± 4.4% (drought) to 80 ± 2.4% at LVB. At LWA there was no significant change in the mean (74.1 ± 20.5% vs. 76.4 ± 5.0%). The greater increase in percent fines in Little Holland Tract than in Liberty Island is likely the result of the greater proximity of Little Holland Tract to the Yolo Bypass. The depletion of fines during the drought suggests the preferential resuspension of fines by wind waves and subsequent export (winnowing).

Dry bulk density was lower near the sediment surface than at depth, and was more variable over time, especially at the Little Holland Tract stations. Bulk density was greater than 0.95 g cm^{-3} in all samples taken from below 4 cm beneath

https://doi.org/10.15447/sfews.2023v21iss1art4

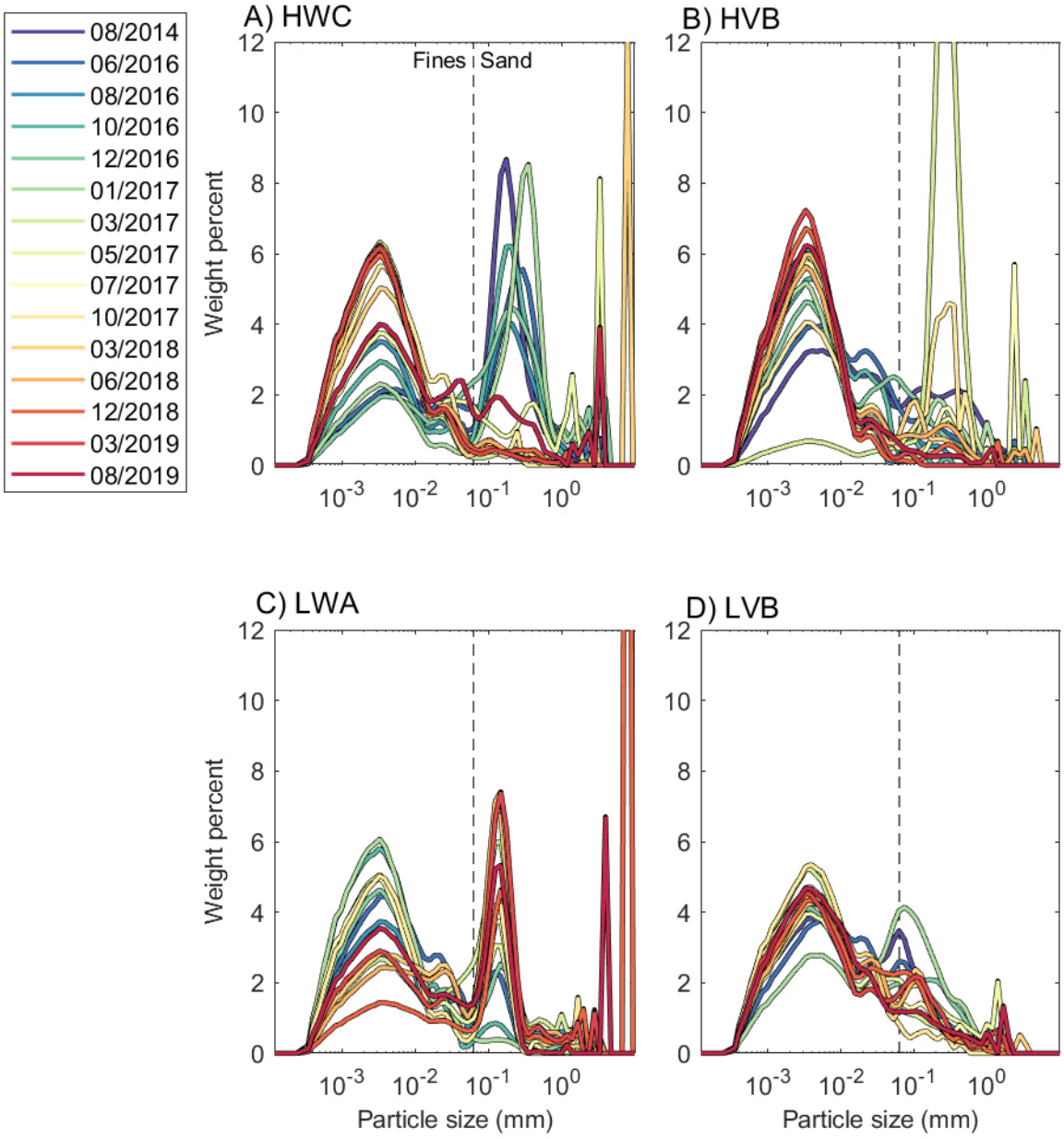

Figure 2 Grain size distribution of surficial bed sediments from samples collected between August 2014 and August 2019 at (**A**) HWC, (**B**) HVB, (**C**) LWA, (**D**) LVB

the sediment–water interface (Figure 4). After the high flows (October 2017), bulk density in the top 2 cm of push cores from HWC, HVB, and LVB was lower than in June 2016, whereas there was little change in bulk density at LWA. The relatively high percent fines at these stations after the 2017 high flows likely contributed to the lower bulk density, because sediment bulk density is usually inversely related to mud content (Flemming and Delafontaine 2000). However, the gradual increase in surficial dry bulk density in 2018 and 2019, when percent fines was relatively stable, suggests that compaction also influenced bulk density. Less compaction in late 2017 indicates that deposition of either resuspended or imported sediment (or both) occurred during or after the high flows. Both the lower percentage of fines and the higher bulk density in 2015–2016 than

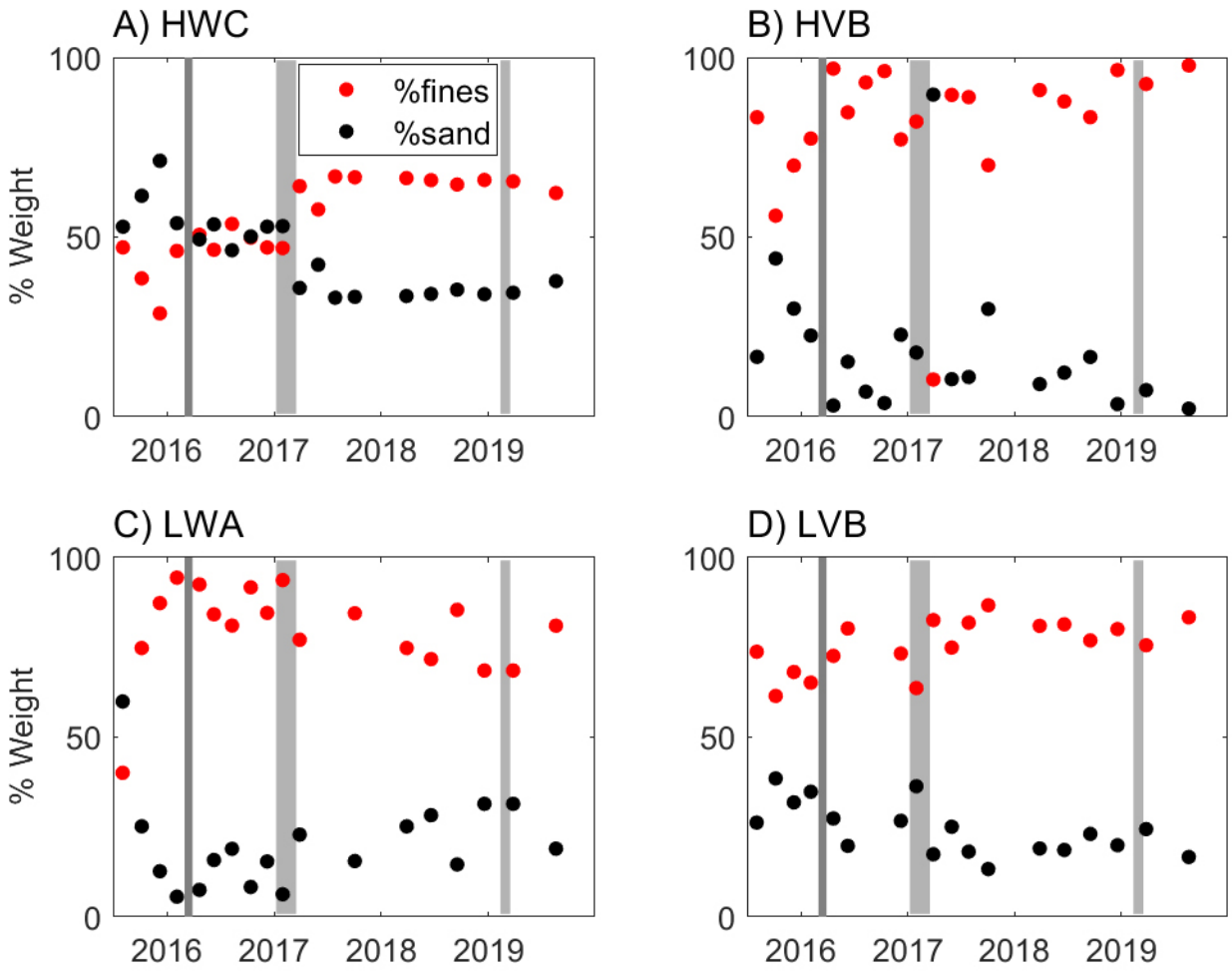

Figure 3 Percent fines (*red*) and sand (*black*) in surficial bed sediments from samples collected between August 2015 and August 2019 at (**A**) HWA or HWC, (**B**) HVB, (**C**) LWA, and (**D**) LVB, with periods of discharge greater than 100 $m^3 s^{-1}$ through the Yolo Bypass (near Woodland) indicated by *shading*.

in October 2017 suggest that the resuspension response to wave shear stress is less in Little Holland Tract during drought conditions than after high flows.

Waves

Average wave height was greater during the summer than the winter period (Figure 5). Wave height was greater in Liberty Island than in Little Holland Tract, consistent with the greater fetch and greater water depth in Liberty Island. Average significant wave heights at HWC and LWA were 0.06 m and 0.11 m, and maximum significant wave heights were 0.38 m and 0.55 m, respectively. Wave period was directly related to wave height, with maximum values of 2 s at HWC and 2.5 s at LWA. In both embayments, wave height was greater at the northern (typically downwind) station (Figure 6). At all stations, wave heights were greater at high than at low tide. Wave orbital motions decrease with depth below the surface, so at low water depths frictional dissipation at the bed increases, reducing wave height. This interaction with the bed can resuspend sediment.

Wind

Winds predominantly originated from the southwest, south, and southeast (Figure 7). The strongest wind was from the southeast during January 2016 at 18 m s^{-1}. During the winter, wind direction was variable, with many events from the northerly quadrants. Wind was on average stronger and more consistently from

https://doi.org/10.15447/sfews.2023v21iss1art4

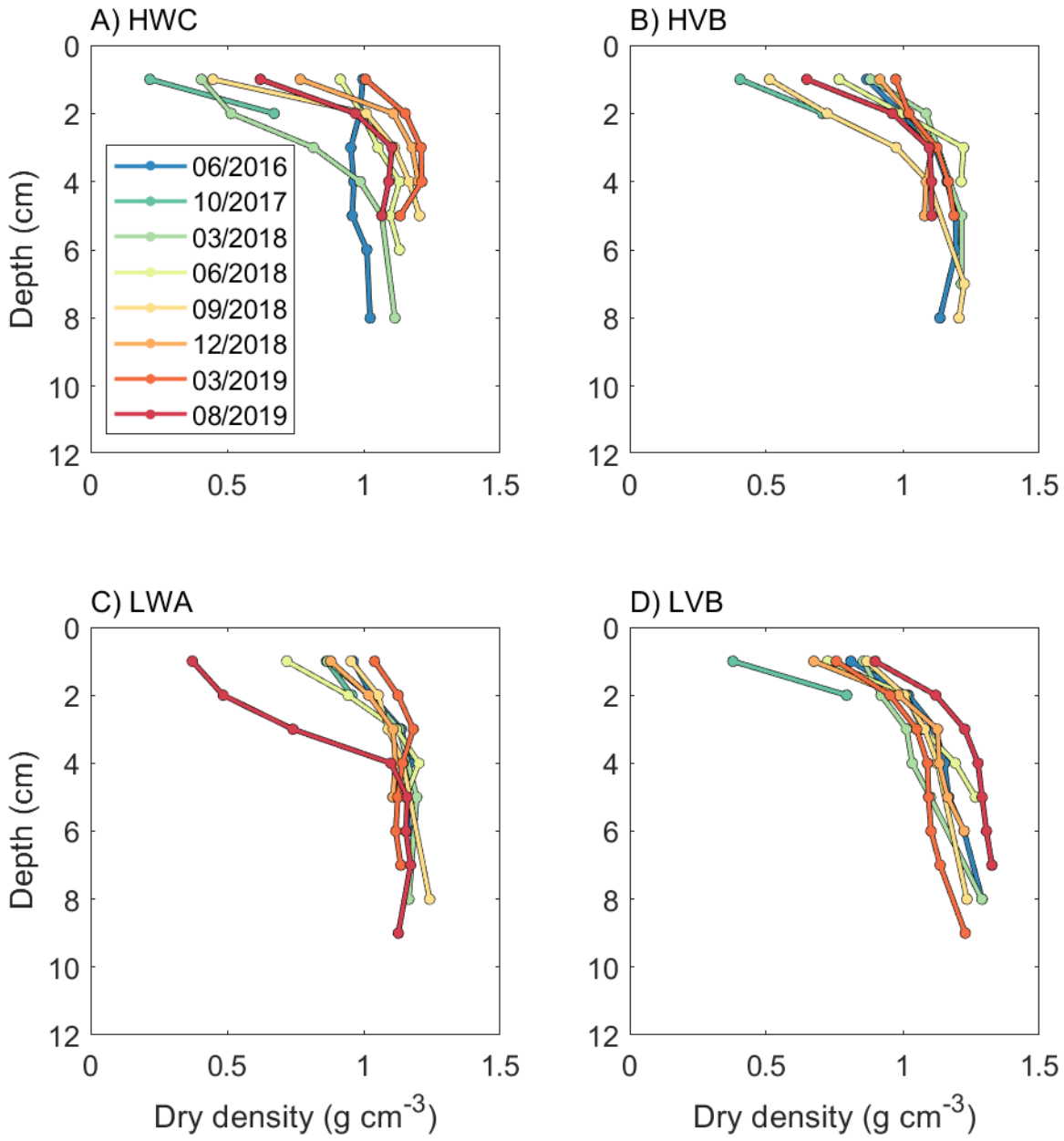

Figure 4 Vertical profiles of dry bulk density in push cores of bed sediments on eight sampling dates at (**A**) HWC, (**B**) HVB, (**C**) LWA, and (**D**) LVB. Depth denotes distance below the sediment–water interface.

the southwest during the summer, with far fewer northerly events, consistent with regional climatology. Sustained high wind speed correlated with peaks in tidally averaged wave height in Liberty Island and Little Holland Tract, and the increase in average wind speed and southwesterly origin in the summer corresponded with an overall increase in wave activity, water level, and SSC.

Suspended-Sediment Concentration

Suspended-sediment concentration varied on the tidal time-scale at all measurement locations within Little Holland Tract and Liberty Island, with higher SSC values at either maximum ebb

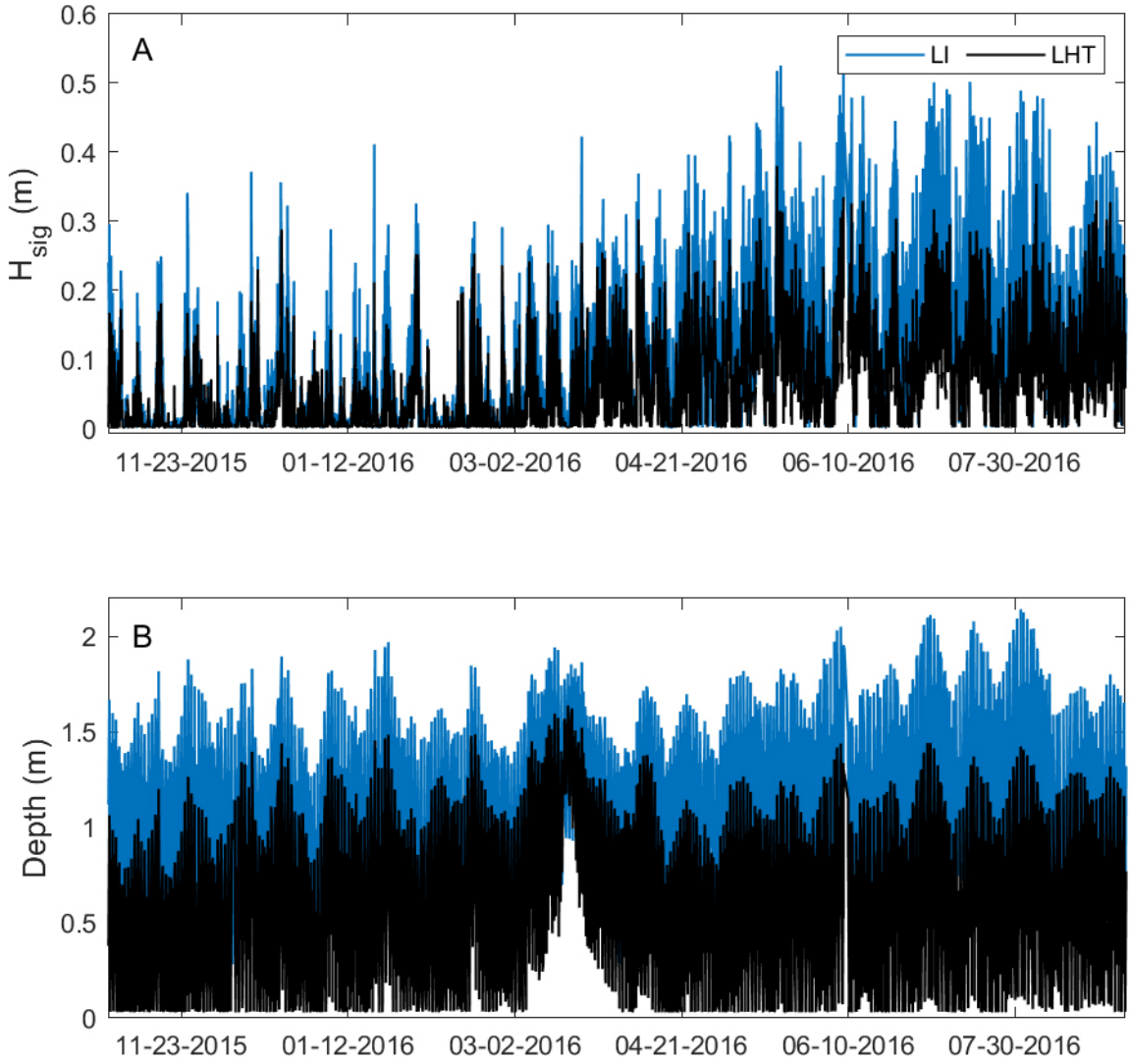

Figure 5 Time-series of (**A**) significant wave height (H_{sig}) and (**B**) water depth at HWC in Little Holland Tract and LWA in Liberty Island from November 2015 to August 2016.

current (HVB) or at low tide (HWC). SSC was usually higher inside Little Holland Tract than Liberty Island, likely because of the greater water depths in Liberty Island (Figure 8). On longer (tidally averaged) time-scales, elevated SSC correlated with periods of lower water depths and prolonged wind–wave events. Average SSC was greater inside Little Holland Tract than at the breaches, and greater at HWC than at HVB (Table 3). HWC is closer to the northern, shallow part of Little Holland Tract, and so is more influenced by wave-driven resuspension than HVB, where mean water depth is greater. Suspended-sediment concentration was greater in summer than in winter at all sites that had data from both periods.

The best predictive model for SSC in Little Holland Tract (stations HVB and HWC) includes the variables depth, tide (a factor that indicates flood or ebb tidal phase), and τ_w. LER values for all the other models are greater than 2, indicating decisive support for the best model (Table 4). SSC is inversely related to depth and directly related to wave shear stress. Although, in principle, resuspension is driven by combined bed shear

https://doi.org/10.15447/sfews.2023v21iss1art4

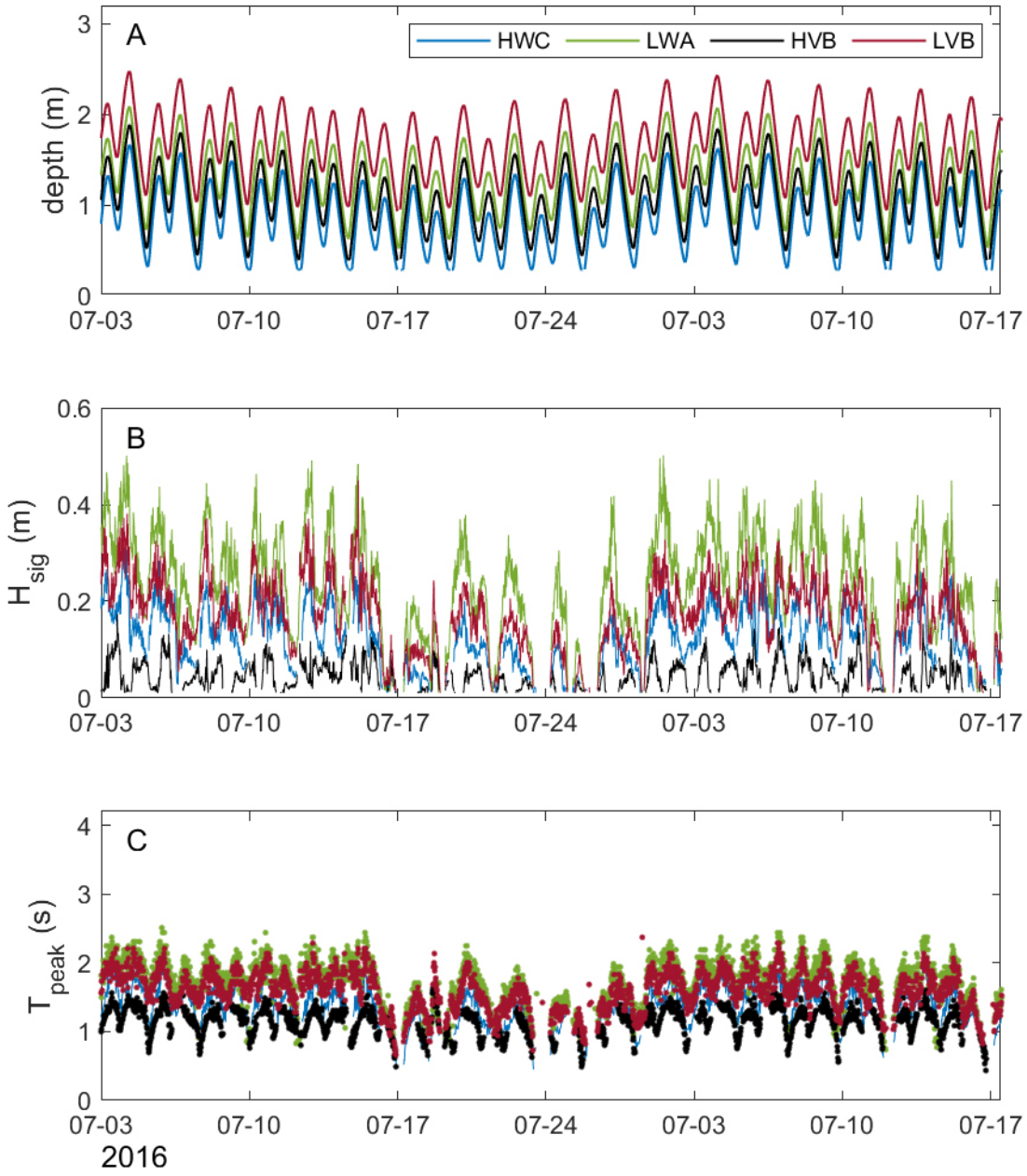

Figure 6 Time-series of (**A**) water depth, (**B**) significant wave height (H_{sig}), and (**C**) wave period measured at HWC, LWA, HVB, and LVB, July 3–17, 2016

stress τ_{wc}, the LER values indicate decisive evidence for the model with τ_w.

The single factor with strongest predictive capability is τ_w, and depth alone accounted for almost as much of the variation. Waves of a given height and period exert greater shear force on the bed in shallower water, but that effect is accounted for by using wave shear stress rather than wave height as a factor. We attribute the improvement in predictive capability from including depth as a factor to the reduction in vertical mixing at low water depths: in these shallow depths, resuspended sediment is distributed over the entire water column, and the volume available for redistribution decreases with water depth (MacVean and Lacy 2014). Another possible explanation is the advection of more

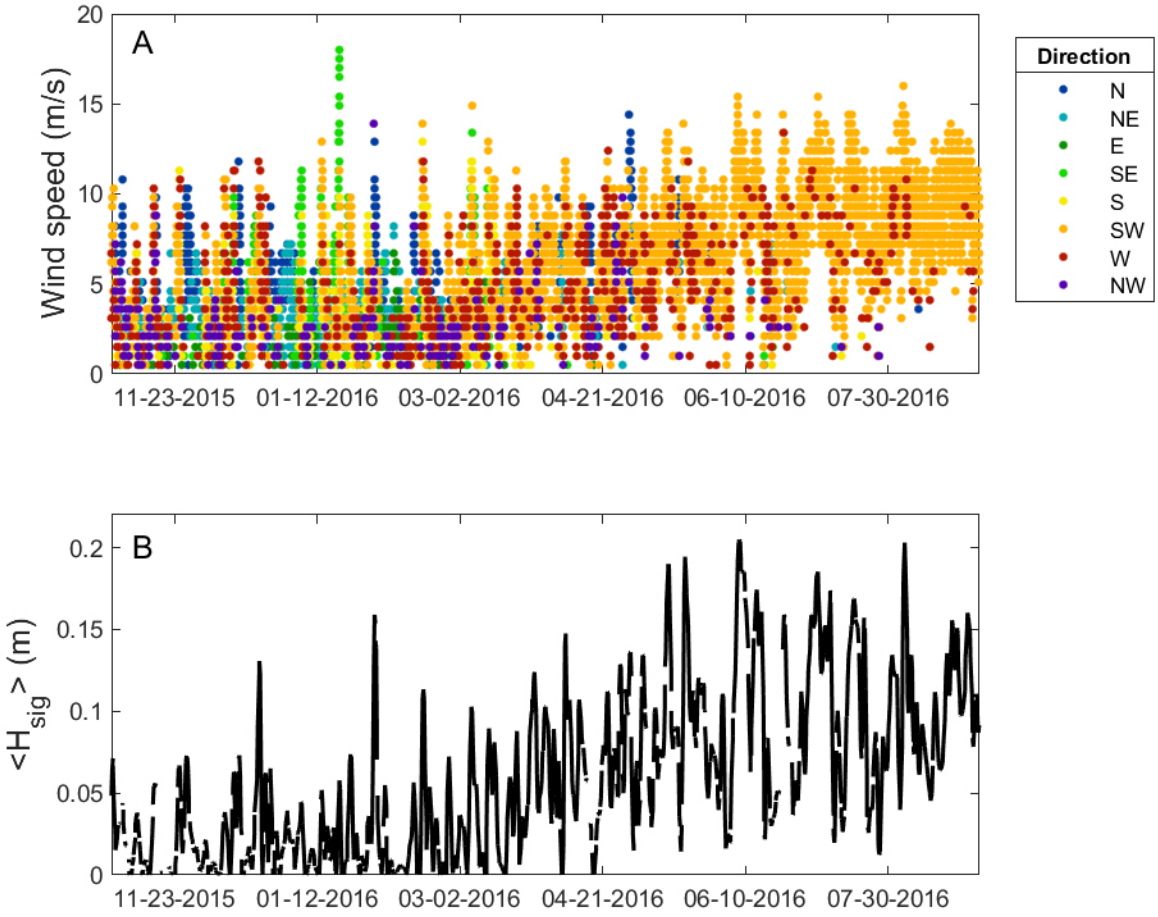

Figure 7 (**A**) Wind speed and direction (indicated by *color*) measured at Travis Air Force Base and (**B**) tidally averaged significant wave height at HWC

turbid water from the northern region of Little Holland Tract (where depth is lower and thus τ_w is greater) during ebb tides, as water level at the stations decreased.

Seasonal Suspended-Sediment Flux

The majority of water and sediment flux to Little Holland Tract pass through the large breach at the South Breach (Figure 1). Flow through the numerous (uninstrumented) small levee breaches is likely a significant component of the water balance (particularly during high river discharge) and may be important to the sediment balance as well. Nevertheless, the mechanisms of seasonal and event-scale SSF through the South and North breaches can be used to identify conditions conducive to sediment export and import. Both the direction and magnitude of tidally averaged water discharge and SSF at the South Breach fluctuated with freshwater inflow and wind events (Figure 9). To explore seasonal patterns in flux driven by tidal and wind-driven processes, we defined winter (November 15, 2015 to March 12, 2016) and summer (April 1 to September 1, 2016) periods, excluding the high flows in late March 2016 (see "Methods"). The winter SSF period starts later than the period used for Table 3 because SSC data are not available for South Breach from September 12 to November 12, 2015. In addition, discharge data (and thus SSF) are not available for the North Breach from November 1 to December 15, 2015 or for April 1 to September 1, 2016.

Cumulatively over the winter period, both the South and North breaches exported sediment: approximately 1,775 MT and 175 MT, respectively (Figure 10). Cumulative ⟨SSF⟩ was primarily

https://doi.org/10.15447/sfews.2023v21iss1art4

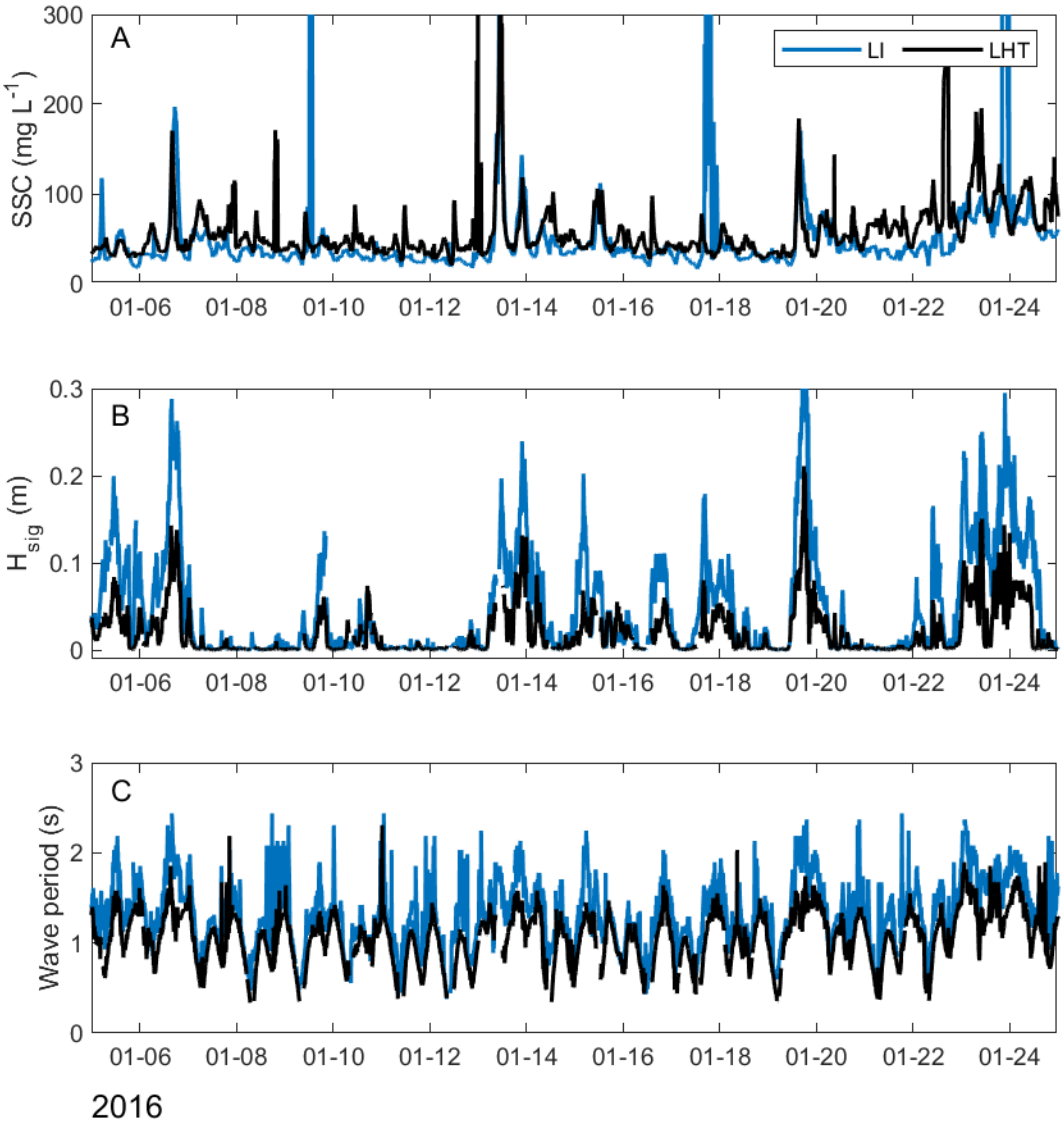

Figure 8 (**A**) Suspended-sediment concentration (SSC) (**B**) significant wave height (H_{sig}) and (**C**) wave period at LWA in Liberty Island and HWC in Little Holland Tract during 20 days in January 2016.

Table 3 Average and standard deviation (σ) SSC for all (winter and summer); winter (September 1, 2015 to March 12, 2016, or November 12, 2015 to March 12, 2016 at South Breach); and summer (April 1 to September 1, 2016), in mg L^{-1}

	All		Winter		Summer	
Station ID	**mean**	**σ**	**mean**	**σ**	**mean**	**σ**
HWC	78	67	67	77	87	56
HVB	58	34	41	31	72	29
South Breach	48	36	36	39	60	30
North Breach	52	35	35	28	69	33
LWA	68	97	52	95	84	96
LVB	39	31	28	28	50	29

advective at the South Breach during the winter period, when increased river flows produced net down-estuary water discharge and elevated SSC in the Toe Drain. The positive advective ⟨SSF⟩ was somewhat offset by a negative (import) dispersive component (−639 MT). At the North Breach, both advective and dispersive ⟨SSF⟩ exported sediment cumulatively over the winter period, although there were periods of import for each component. Cumulative dispersive ⟨SSF⟩ at the North Breach (117 MT) was more than double advective (57 MT), indicating the importance of export produced by greater ⟨SSF⟩ within Little Holland Tract than in

Table 4 AIC scores and log evidence ratio (LER) values for eleven models based on combined data from HWC and HVB, showing AIC value corrected for sample size (AICc), the change in AICc compared to the best model (ΔAICc), the relative weight of AICc values (w_i), and the pseudo R^2 value for each model *i*. All models had non-zero intercepts.

AICc	ΔAICc		LER	model	Psuedo R^2
38672	0.0	1.00	0.0	ssc ~ depth + tide + τ_w	0.45
38885	213.0	$<<1e^{-4}$	46.3	ssc ~ depth + τ_w	0.42
38978	305.3	$<<1e^{-4}$	66.3	ssc ~ depth + tide + τ_{wc}	0.41
39159	486.1	$<<1e^{-4}$	105.6	ssc ~ depth + τ_{wc}	0.38
39357	685.0	$<<1e^{-4}$	148.7	ssc ~ depth + tide + τ_c	0.35
39360	687.3	$<<1e^{-4}$	149.3	ssc ~ depth + tide	0.35
39489	816.6	$<<1e^{-4}$	177.3	ssc ~ τ_w	0.33
39585	912.8	$<<1e^{-4}$	198.2	ssc ~ depth	0.31
39746	1073.9	$<<1e^{-4}$	233.2	ssc ~ τ_{wc}	0.28
40735	2062.1	$<<1e^{-4}$	NA	ssc ~ τ_c	0.08
41082	2409.7	$<<1e^{-4}$	NA	ssc ~ tide	0.00

adjacent channels, and contrasting with the South Breach where dispersive ⟨SSF⟩ imported sediment.

During the summer, there was cumulative import of suspended sediment at the South Breach (–1,321 MT) (Figure 11). Both advective and dispersive components of ⟨SSF⟩ were negative, and as in the winter period, advective ⟨SSF⟩ dominated. This cumulative import of suspended sediment is consistent with the landward sediment-transport pattern that has been observed throughout the Cache Slough complex in dry conditions (Morgan–King and Schoellhamer 2013). The change in sign of the slope of cumulative ⟨SSF⟩ in early May 2016—indicating a shift from sediment export to import through the South Breach—coincides with the onset of greater wave heights (Figure 11).

For the combined winter and summer, there was net sediment export at the South Breach (455 MT). In addition, during the large river flow event in mid-March 2016 (which was excluded), sediment was certainly exported, because discharge at the South Breach was continuously down-estuary. In the winter, cumulative ⟨SSF⟩ was dominated by short pulses of export (e.g., February 1, Figure 10), whereas after May 1 ⟨SSF⟩ was relatively constant, as shown by the slope in cumulative ⟨SSF⟩. The winter pulses coincided with northerly winds and net export of water (positive ⟨*Q*⟩) (Figures 9 and 12). Northerly wind events also corresponded to peaks in export from the South Breach in summer, but they occurred less frequently (especially after May 1) and, unlike in winter, were not associated with increased river flow. The summer export pulses were offset by long periods of import, so they accounted for less of the total ⟨SSF⟩ than in winter (Figure 12).

Cumulative seasonal ⟨SSF⟩ at the Little Holland Tract South breach was dominated by regional trends in sediment transport: export in winter from increased river flows and import in summer. The cumulative tidally averaged import in summer—which is the season of strongest winds—indicates that wind-wave resuspension coupled with concentration-gradient-driven transport does not dominate SSF dynamics. Instead, Little Holland Tract was a sediment sink in summer.

Wind-Wave Events

We explored the extent to which wind-wave resuspension exports suspended sediment on event time-scales, despite its lack of influence on the seasonal pattern of SSF. Three wave events illustrate how winds and wind waves influence the magnitude and direction of ⟨SSF⟩ at the two Little Holland Tract breaches and the southern Liberty Island breach, and the potential for short-

https://doi.org/10.15447/sfews.2023v21iss1art4

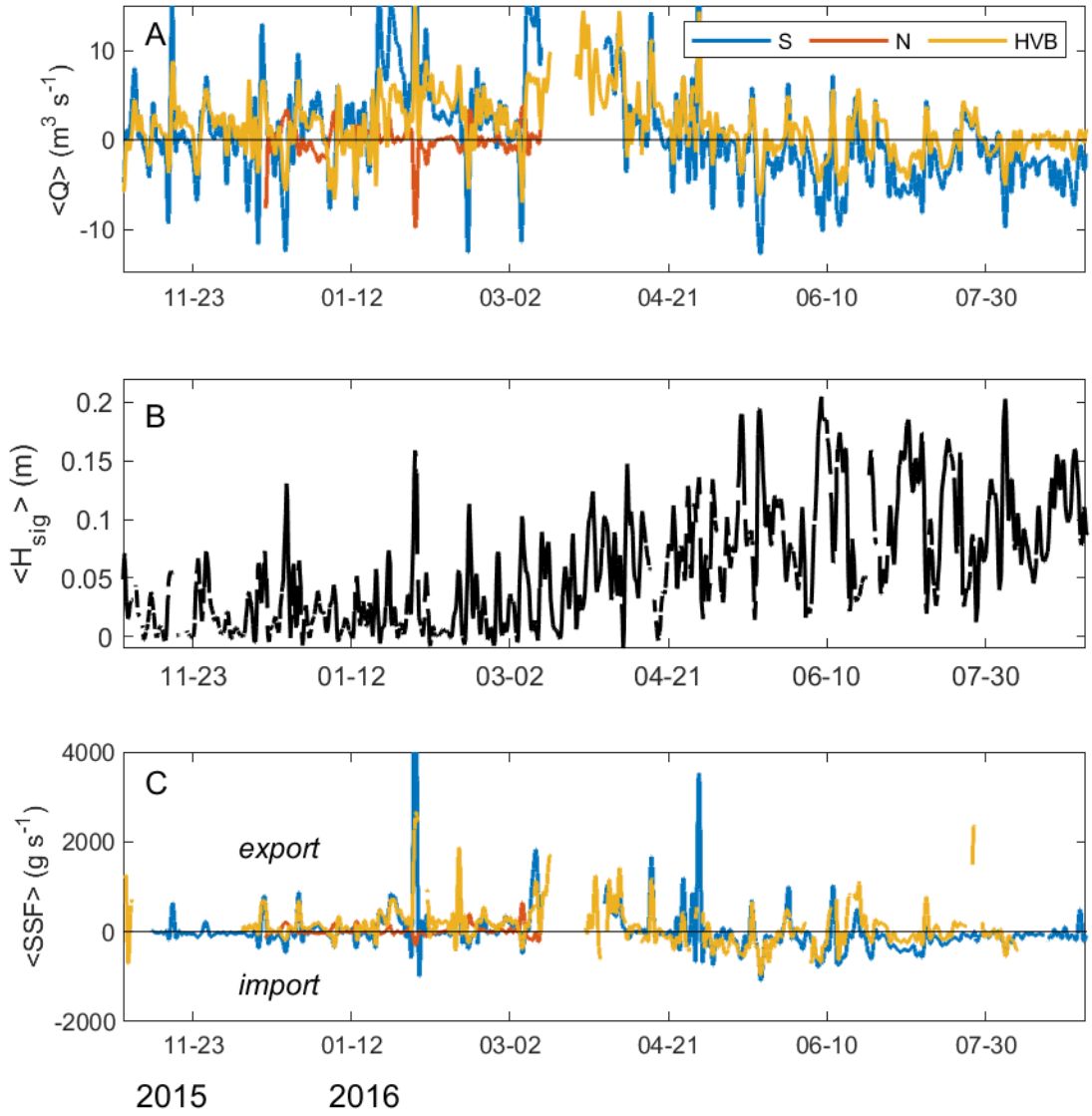

Figure 9 Time-series of tidally averaged (**A**) discharge (Q), (**B**) significant wave height (H_{sig}) at HWC, and (**C**) suspended-sediment flux (SSF) at South Breach (S), North Breach (N), and HVB stations in Little Holland Tract. Export (ebb direction) positive; *brackets* denote tidal average.

term sediment export (Figure 13). We include ⟨SSF⟩ from LIB in this section because Liberty Island, as a result of its greater volume, has much greater potential than Little Holland Tract to influence surrounding waters. Other than during large outflow events, ⟨Q⟩ shows that water is consistently imported at LIB, which indicates that there must be significant tidally averaged export of water through other unmeasured breaches and suggests that the consistent tidally averaged import of sediment at LIB does not represent the entire sediment budget of Liberty Island. Nevertheless, the LIB data are relevant to our focus on changes in magnitude and direction of ⟨SSF⟩ attributable to wind–wave events. Results from HVB are also included, primarily to demonstrate consistency with South Breach.

During the first event, wave height peaked on December 23, 2015, followed by two smaller wave peaks on December 24 and 26 (Figure 13). The first two peaks were produced by southerly winds, and on December 26 the wind changed direction to northerly (Figure 13, bottom panel). Sediment

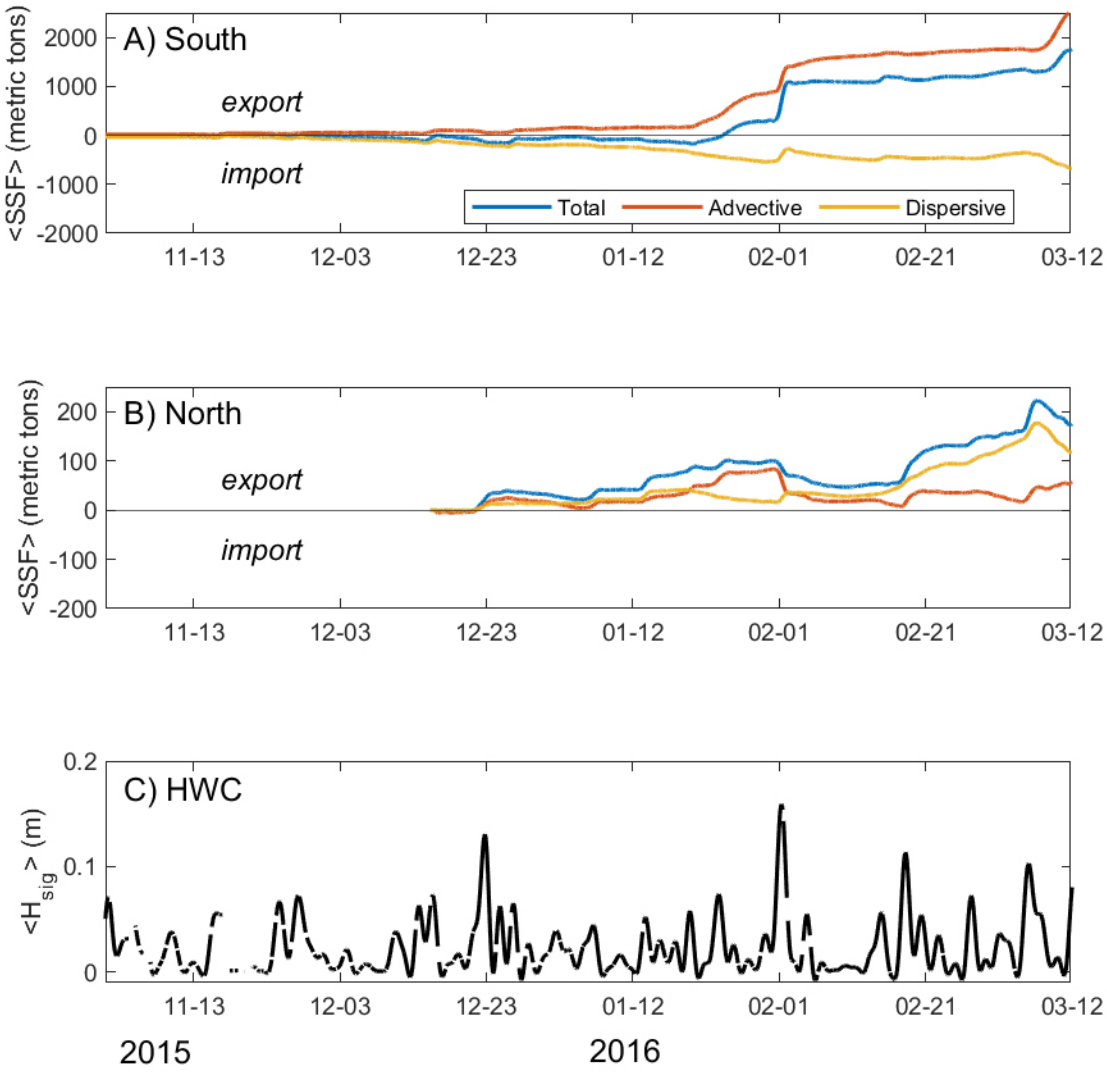

Figure 10 Cumulative total, advective, and dispersive suspended-sediment flux (SSF) at (**A**) South Breach and (**B**) North Breach in Little Holland Tract, and (**C**) tidally averaged significant wave height (H_{sig}) at HWC from November 2015 to March 12, 2016. Export (ebb direction) positive; *brackets* denote tidal average.

was imported (negative ⟨SSF⟩) through the South and LIB breaches during the first wave peak, as tidally averaged import of water ⟨*Q*⟩ caused by southerly wind and waves drove an increase in tidally averaged water depth (set up). These same conditions produced an increase in ⟨SSC⟩ and a small export of ⟨SSF⟩ at the North Breach. Note that maximum ⟨SSC⟩ in Little Holland Tract, as represented by station HWC, coincided with the maximum wave height, but occurred later than the sediment import pulse at South. The second (lower) southerly wave peak kept the water level high, but the third northerly peak (December 26) produced a drop in water level of more than 30 cm, which exported sediment, with the greatest magnitude of the 7-day period. Wind speed and wave heights during the final ⟨SSF⟩ pulse were moderate: the pulse was produced by the combination of Little Holland Tract draining during wind relaxation and elevated SSC from prior wind-wave resuspension. The net flux for this 7-day period was low because the initial import offset the subsequent export: in Little Holland Tract net ⟨SSF⟩ totaled –19 MT at the South Breach, and 37 MT at the North breach. Although each peak was much greater in

https://doi.org/10.15447/sfews.2023v21iss1art4

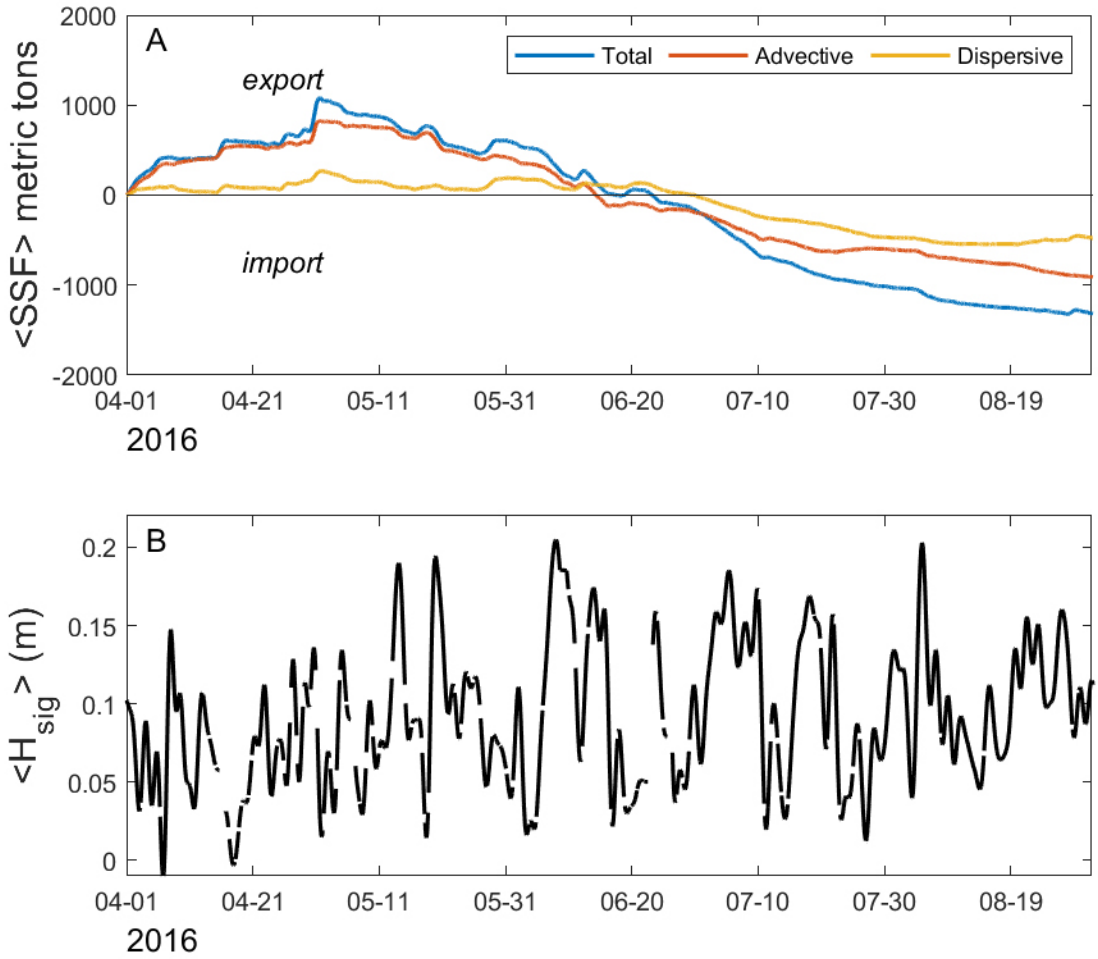

Figure 11 (**A**) Cumulative total, advective, and dispersive suspended-sediment flux (SSF) at South Breach in Little Holland Tract and (**B**) tidally averaged significant wave height (H_{sig}) at HWC during the summer period (April 1 to September 1 2016). Export (ebb direction) positive; *brackets* denote tidal average.

magnitude at South Breach than North Breach, the total for the period was greater at North Breach. At LIB, ⟨SSF⟩ followed a similar temporal pattern to South Breach, but the initial import from set up was much greater, resulting in a net sediment import.

The second event, which spanned January 30 to February 3, 2016, had a single peak in wave height produced by a short period of relatively strong northerly winds. Water level dropped during the wind event (set down), and SSC peaked at all instrument locations, resulting in a large export peak in ⟨SSF⟩ at the southern breaches of Little Holland Tract and Liberty Island. Sediment was imported—and the magnitude of ⟨SSF⟩ was much lower—at the North Breach, where set down is expected to produce net inflow. Cumulative SSF totaled 634 MT at the South Breach, accounting for about 40% of the cumulative SSF during the winter, −30 MT at the North breach, and 492 MT at LIB. Peak ⟨SSF⟩ was greater at LIB than at South Breach because of the greater volume of Liberty Island, but the sediment export was offset by import before and after the wind event. River flow increased during this winter event, contributing to ⟨SSF⟩ export at South Breach and LIB, and potentially supplying sediment (through unmonitored breaches) to Liberty Island and Little Holland Tract as well, so that some of the ⟨SSF⟩ measured at South Breach may have passed *through* Little Holland Tract rather than originating there.

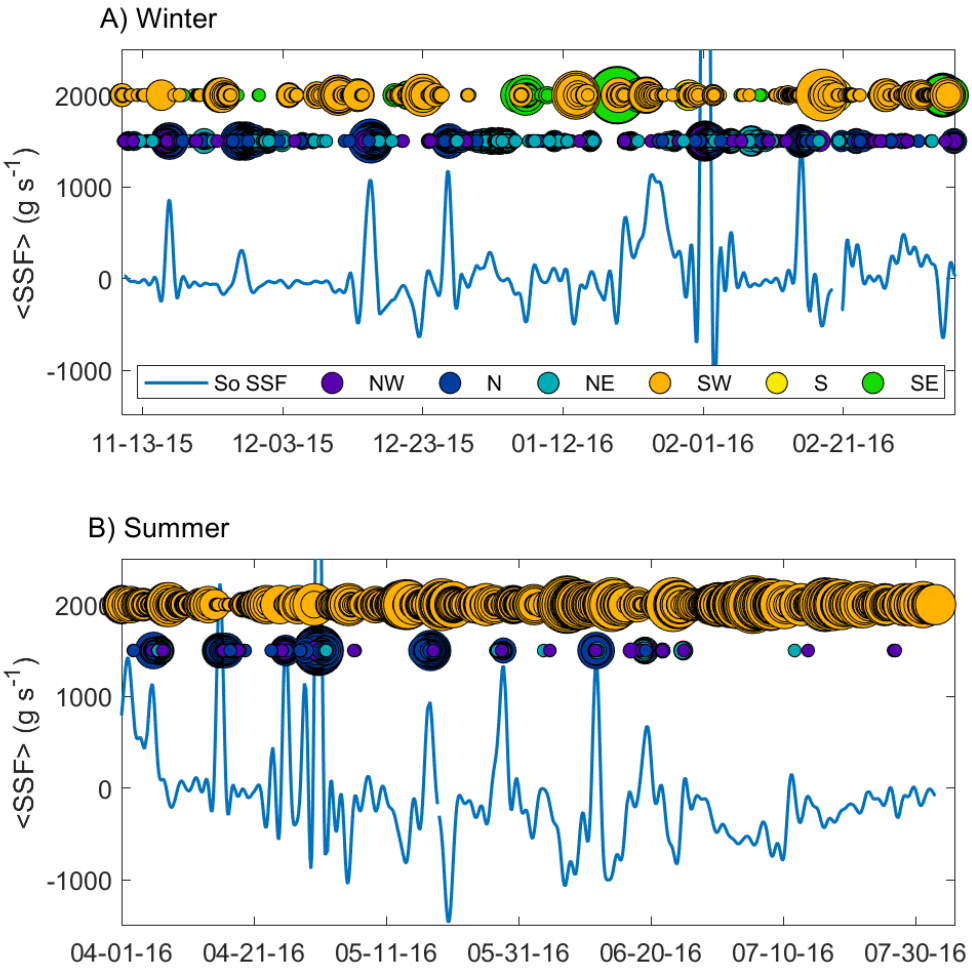

Figure 12 Tidally averaged suspended-sediment flux at Little Holland Tract South Breach and wind statistics measured at Travis Air Force Base for (**A**) winter and (**B**) summer periods. *Circle size* scaled to wind speed; *circle color* denotes wind direction. Export (ebb direction) positive for SSF.

During the third period, May 11 through 23, 2016, there were two large southerly wave peaks, both associated with pulses of ⟨SSF⟩ import at South Breach (discharge data are not available from the North Breach for these dates). Sediment was exported at South Breach in between these two peaks, when the winds and waves relaxed and the water level dropped. The pattern of ⟨SSF⟩ response to the wind events was the same at LIB but superimposed on tidally averaged import of sediment produced by flood-directed ⟨*Q*⟩ at this site. Cumulatively, suspended sediment was imported at South Breach during this period (341.72 MT).

In summary, at South Breach, during southerly wind events sediment export was driven by basin draining as winds subsided after the event and was offset by sediment import as wind and wave set up filled the basin. These events either imported sediment or resulted in near-zero SSF, depending on the sequence of filling and draining, and the persistence of the elevated SSC due to wind waves. The same dynamics exported sediment (during the December event) through the North Breach where set up generates export of water and elevated SSC within Little Holland Tract can produce export through dispersive SSF. Northerly wind-wave events cause set down rather than set up, so maximum SSC and maximum discharge coincide, exporting large quantities of suspended sediment through the South Breach and LIB.

https://doi.org/10.15447/sfews.2023v21iss1art4

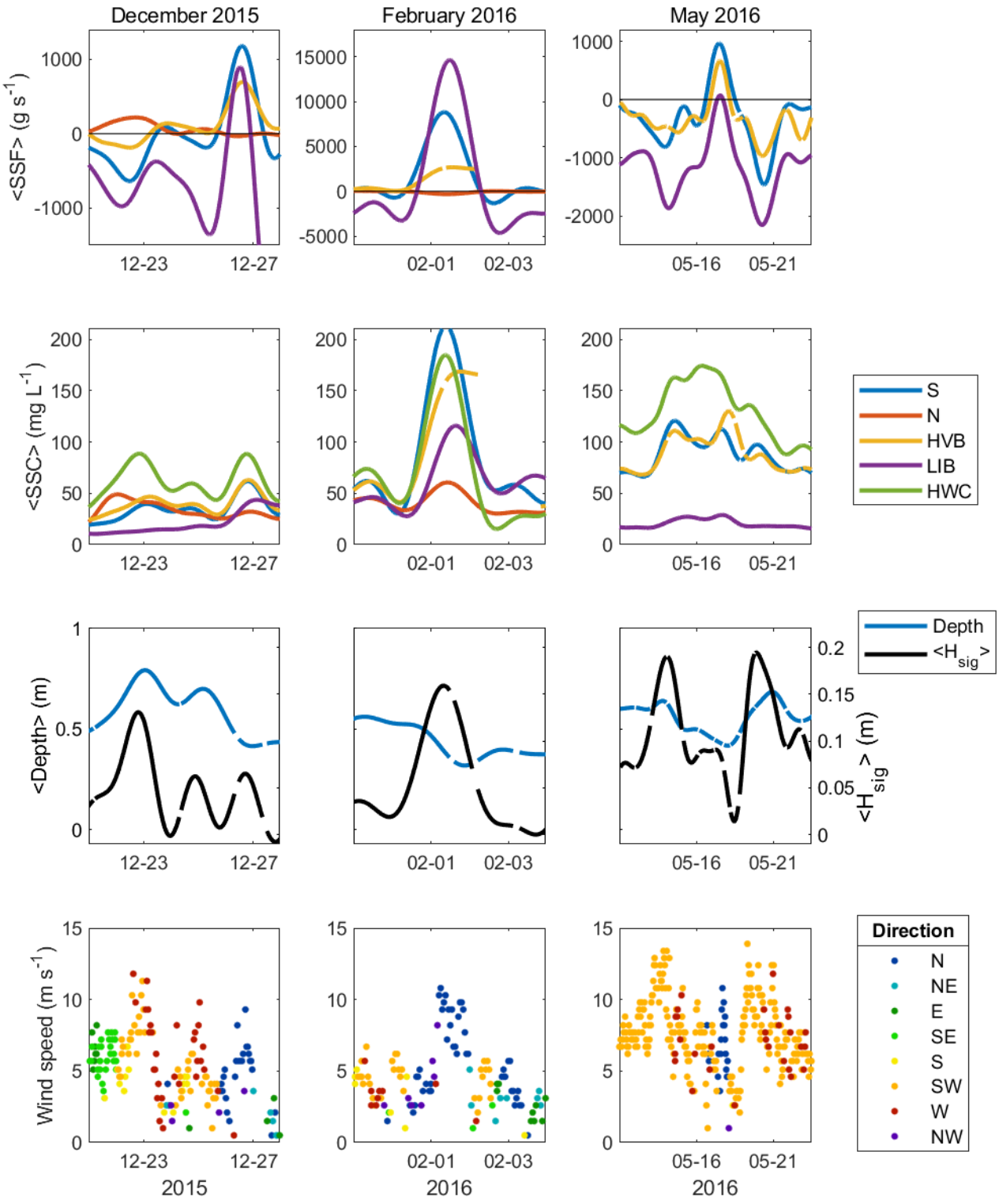

Figure 13 Suspended-sediment flux (SSF) at four sites (**row 1**; export positive), suspended-sediment concentration (SSC) at five sites (**row 2**), water depth and significant wave height (H_{sig}) at HWC (**row 3**), and wind speed and direction measured at Travis Air Force Base (**row 4**) during three wind events (*identified by column headings*). *Brackets* denote tidal average.

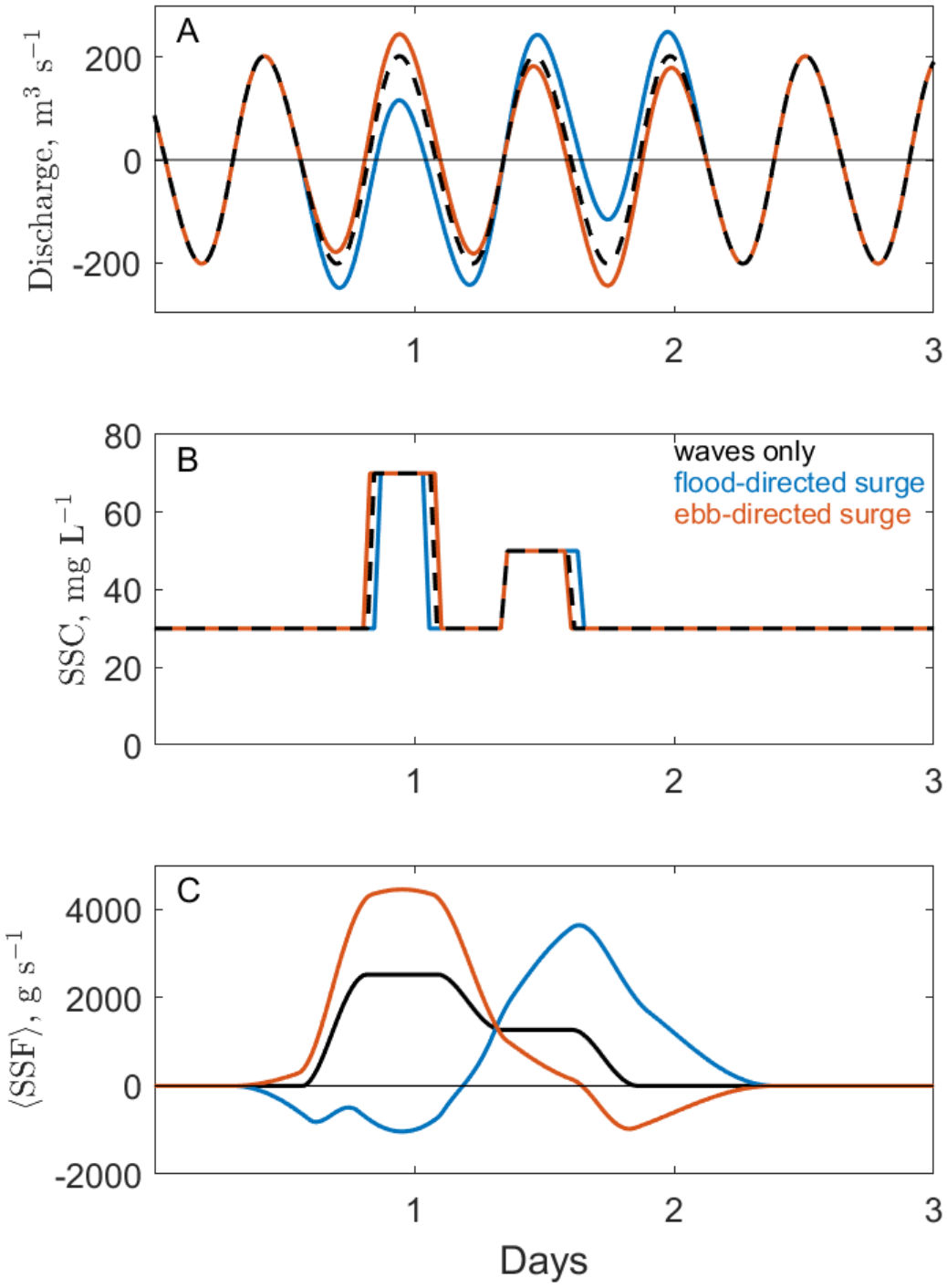

Figure 14 (**A**) Discharge, (**B**) suspended-sediment concentration (SSC), and (**C**) tidally averaged suspended-sediment flux from analytical model of three cases: waves only (Case 1, *black*), waves and flood-directed surge (Case 2, *blue*), and waves and ebb-directed surge (Case 3, *red*). Export (ebb direction) positive; *brackets* denote tidal average.

https://doi.org/10.15447/sfews.2023v21iss1art4

DISCUSSION

Mechanisms of Sediment Export from Shallow Basins

On a seasonal time-scale, tidally averaged SSF from Little Holland Tract was dominated by regional advective flux: export in winter, driven by elevated river discharge, and import in summer, driven by flood-dominated tidal asymmetry and sediment trapping in shallows (Morgan–King and Schoellhamer 2013). Sediment transported into shallow basins such as Little Holland Tract and Liberty Island by the flood-dominated tides of summer tends to settle in the lower-velocity basin waters, resulting in net import.

In shallow basins such as Little Holland Tract, strong winds produce wind waves that increase bed shear stress, resulting in sediment resuspension and higher turbidity than in deeper waters. We observed two distinct mechanisms for export of this suspended sediment from a shallow tidal basin connected to surrounding waters by discrete breaches, which operate on the time-scale of wind-wave events (3 to 4 days). The first is a dispersive mechanism: because of the turbidity gradient between the basin and surrounding channels, SSF is greater on ebb than flood tides. The second mechanism is advective, driven by wind and wave set up and relaxation.

We explored the relative importance of these two mechanisms with a simple analytical model of SSF through the breach of an idealized basin–breach system (Figure 14). In this system, flow through the breach is primarily driven by semidiurnal tides (period 12.5 hours), and the basin is well mixed, with no spatial variability in SSC. During calm conditions, SSC during both flood and ebb tides (representing outside and within the basin) is 30 mg L^{-1}. Starting at 0.75 days and persisting for 1.5 tidal cycles, SSC during ebb tides increases to 70 mg L^{-1}, representing windy conditions; and during the following ebb tide SSC is 50 mg L^{-1}, corresponding to the persistence of fine sediments in suspension after resuspension (Figure 14B). In Case 1 (termed waves only), the only effect of the winds is the increased SSC during ebb tides, isolating the dispersive mechanism of SSF. The other two cases include the advective mechanism of wind and wave set up in addition to the dispersive mechanism. In Case 2, a negative sinusoidal surge in discharge (20 m^3 s^{-1} amplitude, 37.5-hour period) is superimposed on the tidal flow in the breach (Figure 14A, blue line), representing flood-directed winds and set up. In Case 3, the sign of the surge is switched, to represent ebb-directed winds and set down; the amplitude of the ebb-directed surge is half that of the Case 2 flood-directed surge. In addition to affecting the tidally averaged discharge, the surges affect the length of the ebb tides, as seen in Figure 14B.

All three cases produce net sediment export (positive ⟨SSF⟩) over 3 days (Figure 14C). Case 1 produces continual export of ⟨SSF⟩, which is entirely dispersive, since ⟨Q⟩ (and thus advective flux) is zero. Maximum SSF coincides with the ebb tide during or immediately after the strongest winds and greatest SSC in the basin. In Case 2 (flood-directed surge), the net import of sediment-laden water over the tidal cycle initially produces tidally averaged import of sediment, even though SSC is lower outside the basin than within. The greatest SSC within the basin coincides with the strongest winds and the highest water level, but not with the greatest export. The relaxation of the wind set up generates export of ⟨Q⟩ and ⟨SSF⟩, which occurs after the maximum SSC. The result is lower cumulative ⟨SSF⟩ over 3 days than for Case 1 (127 MT vs. 170 MT). In Case 3 (ebb-directed surge), maximum ⟨SSF⟩ coincides with the maximum ⟨SSC⟩, so that the dispersive and advective mechanisms reinforce each other to export the most sediment of the three cases (3-day net ⟨SSF⟩ of 201 MT), despite a surge amplitude 50% less than the Case 2 flood-directed surge. Net ⟨SSF⟩ for an ebb-directed surge equal in magnitude to the Case 2 surge is 231 MT.

In the South Breach at Little Holland Tract, the flood-directed surge case corresponds to southerly and southwesterly winds, which occur most days in summer. The ebb-directed surge case corresponds to northerly wind events, which were observed to produce the greatest peaks in sediment export (Figure 11). In winter, northerly events can be associated with local precipitation

and increased export, which increases export at the South Breach, although elevated SSC throughout the Delta during high river flows (rather than resuspension within Little Holland Tract) is likely an important contributor to the largest export peaks in ⟨SSF⟩. Pulses of ⟨SSF⟩ export during summer northerly winds are likely produced by the mechanisms illustrated in Figure 14. In the North Breach, southerly winds produce ⟨*Q*⟩ and ⟨SSF⟩ export, but with much smaller magnitude than at the South Breach (or in the analytical model) because of the small cross-sectional area of the breach (Figure 12, first event).

Configuring Shallows to Optimize Habitat

The higher turbidity produced by wind-wave resuspension in flooded basins in the Delta is beneficial to some native fishes. Two possible management goals for these shallow basins are to maintain turbid conditions within the shallows, or to maximize export of turbidity to improve habitat quality in surrounding waters. These two goals may be mutually exclusive, because increased export of suspended sediment reduces the pool of easily resuspended sediment. Similarly, shallow basins can be designed to maximize either sediment retention or export, or perhaps an optimal design might result in intermittent export during spring tides (Stumpner et al. 2021). SSC in—and the direction of SSF from—shallow basins such as Little Holland Tract depend on interactions of meteorological and hydrodynamic forcing, sediment supply, and basin size and orientation. Among these factors, basin shape, orientation, and depth—as well as breach location—are the most controllable, and sediment supply can also be managed.

Turbidity increases at low tide in shallow basins, both because slower tidal currents enhance deposition, and because more wave energy reaches the bed, increasing wave-driven resuspension. In the extreme, shallow depth decreases habitat quality for fish, caused by high temperatures or drying of intertidal regions at low tide (Sommer and Mejia 2013). Little Holland Tract, despite greater turbidity than surrounding waters in the summer and fall, did not consistently export SSC through the largest breach (South Breach), which was usually upwind in summer. Little Holland Tract exported sediment in winter, but mostly during periods of high river discharge, when much of the exported sediment likely passed through Little Holland Tract rather than originating there. Thus, as currently configured, Little Holland Tract is not improving habitat in surrounding waters by increasing turbidity. Export of SSC to surrounding waters from basins like Little Holland Tract could be increased by positioning large breaches downwind of the more consistent summer wind direction (at the northern end in the case of Little Holland Tract). Tidal prism of the basin is also an important consideration: tracts with larger tidal prisms on the scale of Liberty Island have more potential to influence surrounding waters than smaller tracts such as Little Holland Tract.

Wind waves create turbidity in flooded agricultural tracts in the Delta in part because of the tendency for fine sediments, which are easily resuspended, to accumulate in shallow basins. Submerged aquatic vegetation (SAV), which is widespread in Delta shallows (Hestir et al. 2016), can affect this phenomenon in two ways. The canopy of the vegetation reduces water velocities, increasing sediment deposition and retention within the SAV (Lacy et al. 2021). At the same time, SAV reduces wave energy and bed shear stress from waves (Madsen et al. 2001), decreasing wave-driven sediment resuspension. Thus, in some locations, SAV removal could increase the potential for sediment resuspension and export. Direct sediment addition is another option for increasing the erodible pool of sediment.

CONCLUSIONS

Data collected over 2 years demonstrate that the interior of Little Holland Tract and Liberty Island are more turbid than waters flowing through breaches in the surrounding levees, and that wind-wave resuspension is a significant factor in producing this turbidity. Suspended-sediment concentration in Little Holland Tract and Liberty Island varied on tidal, event, and seasonal time-scales. Average SSC was greater within the basins

https://doi.org/10.15447/sfews.2023v21iss1art4

than in levee breaches connecting to adjacent channels and was greater in the summer than in the winter period. Comparison of linear regression models shows that the single factor that accounted for most of the variation in SSC is bed shear stress from waves, followed by water depth, and that the best predictive model includes these two variables as well as tidal phase.

Surficial bed sediments from Little Holland Tract and Liberty Island comprise mud and fine sand, with the proportion of the two varying between sampling sites and over time. The temporal variation in the composition and bulk density of bed sediments suggests active resuspension, redistribution, and supply during the study period.

There was a net export of suspended sediment in winter and a net import in summer through the South Breach in Little Holland Tract, reflecting regional patterns. Down-estuary SSF in winter is driven by increased river flows, and landward SSF in summer is produced by flood-dominated tidal asymmetry and sediment trapping (Morgan–King and Schoellhamer 2013). In summer, although SSC in Little Holland Tract increased, sediment was imported rather than exported, and thus Little Holland Tract did not increase turbidity in surrounding waters.

Sediment was exported from Little Holland Tract on the time-scale of wind-wave events (3 to 4 days), and we identified two mechanisms for this export: dispersive flux, the result of an increase in the spatial gradient in SSC when waves resuspend sediment, and advective flux, caused by wind and wave set up and relaxation. When a breach is downwind of a basin, maximum advective and dispersive export coincide, enhancing the total. When a breach is located upwind, the set up produces advective import, offsetting the positive dispersive flux, and the advective export during relaxation occurs after the peak in SSC, resulting in a lower total export than for downwind breaches.

Morphologic features—including breach location relative to wind direction, basin tidal prism, and basin depth—affect sediment retention or export from shallow basins, so habitats can be designed and configured to enhance these processes.

ACKNOWLEDGMENTS

Emily Carlson contributed significantly to this project, organizing and participating in most of the data collection, processing most of the data, and contributing to data analysis. We thank Cordell Johnson, Pete DalFerro, Tim Elfers, Dan Powers, Andrew Stevens, and Joanne Ferreira for their support and contributions to the project. Thanks to Jon Burau for motivating this work, and to Larry Brown for input on management implications of the results. This paper benefited from review by Andrea O'Neill of the US Geological Survey and, on behalf of the journal, Dave Schoellhamer and one anonymous reviewer. This work was funded by the Bureau of Reclamation and the US Geological Survey Coastal and Marine Hazards and Resources Program. Any use of trade, product, or firm names in this paper is for descriptive purposes only and does not imply endorsement by the US government.

REFERENCES

Bennett WA, Moyle, PB. 1996. Where have all the fishes gone? Factors producing fish declines in the Sacramento–San Joaquin Estuary. In: Hollibaugh JT, editor. San Francisco Bay: the ecosystem. San Francisco (CA): American Association for the Advancement of Science, Pacific Division. 542 p.

Bever AJ, MacWilliams ML, Herbold B, Brown LR, Feyrer F. 2016. Linking hydrodynamic complexity to Delta Smelt (*Hypomesus transpacificus*) distribution in the San Francisco Estuary, USA. San Franc Estuary Watershed Sci. [accessed 2022 Jan 15];14:3. *https://doi.org/10.15447/sfews.2016v14iss1art3*

Burnham KP, Anderson DR. 2002. Model selection and multimodel inference: a practical information-theoretic approach. 2nd ed. New York (NY): Springer–Verlag. 488 p.

Burnham KP, Anderson DR. 2004. Multimodel inference: understanding AIC and BIC in model selection. Sociol Methods Res. [accessed 2022 Jan 15];33:261–304.

[CNDDB] California Natural Diversity Database. 2023. State and federally listed endangered and threatened animals of California. Sacramento (CA): California Department of Fish and Wildlife. [accessed 2023 Jan 26]. Available from: *https://nrm.dfg.ca.gov/FileHandler.ashx?DocumentID=109405&inline*

Conomos TJ, Smith RE, Gartner JW. 1985. Environmental setting of San Francisco Bay. Hydrobiologia [accessed 2023 Mar 17]; 129:1-12. *https://doi.org/10.1007/BF00048684*

Feyrer F, Nobriga ML, Sommer TR. 2007. Multidecadal trends for three declining fish species: habitat patterns and mechanisms in the San Francisco Estuary, California, USA. Can J Fish Aquat Sci. [accessed 2022 Jan 15];64:723–734. *https://doi.org/10.1139/f07-048*

Fischer HB, List EJ, Koh RCY, Imberger J, Brooks NH. 1979. Mixing in inland and coastal Waters. San Francisco (CA): Academic Press. 483 p.

Flemming BW, Delafontaine MT. 2000. Mass physical properties of muddy intertidal sediments: some applications, misapplications, and non-applications. Cont Shelf Res. [accessed 2022 Nov 14];20:1179–1197. *https://doi.org/10.1016/S0278-4343(00)00018-2*

Fregoso TA, Wang R–F, Alteljevich E, Jaffe BE 2017. San Francisco Bay–Delta bathymetric/topographic digital elevation model (DEM): US Geological Survey data release [accessed 2021 Jun 1]. *https://doi.org/10.5066/F7GH9G27*

Grant WD, Madsen OS. 1979. Combined wave and current interaction with a rough bottom. J Geophys Res Oceans. [accessed 2021 Dec 15];84:1797–1808. *https://doi.org/10.1029/JC084iC04p01797*

Hasenbein M, Komoroske LM, Connon RE, Geist J, Fangue NA. 2013. Turbidity and salinity affect feeding performance and physiological stress in the endangered Delta Smelt. Integr Comp Biol. [accessed 2022 Nov 14];53:620–634. *https://doi.org/10.1093/icb/ict082*

Hestir EL, Schoellhamer DH, Greenberg J, Morgan–King T, Ustin SL. 2016. The effect of submerged aquatic vegetation expansion on a declining turbidity trend in the Sacramento–San Joaquin River Delta. Estuaries Coasts. [accessed 2020 Dec 1];39:1100–1112. *https://doi.org/10.1007/s12237-015-0055-z*

Iowa State University. 2018. Iowa Environmental Mesonet: ASOS Network [accessed 2022 Apr 20]. Available from: *https://mesonet.agron.iastate.edu/request/download.phtml?network=CA_ASOS*

Jassby AD, Cloern JE, Cole BE. 2002. Annual primary production: patterns and mechanisms of change in a nutrient-rich tidal ecosystem. Limnol Oceanogr. [accessed 2022 Mar 1];47(3): 698–712. *https://doi.org/10.4319/lo.2002.47.3.0698*

Jones NL, Thompson JK, Monismith SG. 2008. A note on the effect of wind waves on vertical mixing in Franks Tract, Sacramento–San Joaquin Delta, California. San Franc Estuary Watershed Sci. [accessed 2022 Dec 1];6(2):4. *https://doi.org/10.15447/sfews.2008v6iss2art4*

Kass RE, Raftery AE. 1995. Bayes factors. J Amer Stat Assoc. 90(430):773–795. *https://doi.org/10.1080/01621459.1995.10476572*

Lacy JR, Carlson EM, Ferreira JCT. 2016. Wind-wave and sediment-transport time-series data from Liberty Island and Little Holland Tract, Sacramento–San Joaquin Delta, California, 2015–2017 (ver. 2.0, September 2019): US Geological Survey Data Release. [accessed 2022 Jan 15]. *https://doi.org/10.5066/F73R0R07*

Lacy JR, Dailey ET, Carlson EM. 2020. Bed sediment properties in Little Holland Tract and Liberty Island, Sacramento–San Joaquin Delta, California, 2014 to 2019 (ver. 2.0, May 2020): US Geological Survey Data Release. [accessed 2022 Jan 15]; *https://doi.org/10.5066/F7V1241K*

Lacy JR, Foster–Martinez MR, Allen RM, Drexler JZ. 2021. Influence of invasive submerged aquatic vegetation (*E. densa*) on currents and sediment transport in a freshwater tidal system. Water Resour Res. [accessed 2022 Mar 1];57:e2020WR028789. *https://doi.org/10.1029/2020WR028789*

Lehman PW, Mayr S, Mecum L, Enright C. 2010. The freshwater tidal wetland Liberty Island, CA was both a source and sink of inorganic and organic material to the San Francisco Estuary. Aquat Ecol. [accessed 2022 Jan 15];44:359–372. *https://doi.org/10.1007/s10452-009-9295-y*

Levesque VA, Oberg KA. 2012. Computing discharge using the index velocity method. US Geological Survey Techniques and Methods. Book 3, chapter A23. 148 p. [accessed 2022 Mar 1]. *https://pubs.usgs.gov/tm/3a23/*

Lopez CB, Cloern JE, Shraga TS, Little AJ, Lucas LV, Thompson JK, Burau JR. 2006. Ecological values of shallow-water habitats: implications for the restoration of disturbed ecosystems. Ecosystems. [accessed 2022 Jan 15]; 9:422–440. *https://doi.org/10.1007/s10021-005-0113-7*

Lucas LV, Cloern JE, Thompson JK, Monsen NE. 2002. Functional variability of habitats within the Sacramento–San Joaquin Delta: restoration implications. Ecol Appl. [accessed 2022 Jan 15];12:1528–1547. *https://doi.org/10.1890/1051-0761(2002)012[1528:FVOHWT]2.0.CO;2*

Lucas LV, Sereno DM, Burau JR, Shraga TS, Lopez CB, Stacey MT, Parchevsky KV, Parchevsky VP. 2006. Intradaily variability of water quality in a shallow tidal lagoon: mechanisms and implications. Estuaries Coasts. [accessed 2022 Jan 15];29(5):711–730. *https://doi.org/10.1007/BF02786523*

Luoma SN, Dahn CN, Healey M, Moore JN. 2015. Challenges facing the Sacramento–San Joaquin Delta: complex, chaotic, or simply cantankerous? San Franc Estuary Watershed Sci [accessed 2021 Nov 10];13(3):7. *https://doi.org/10.15447/sfews.2015v13iss3art7*

MacVean LJ, Lacy JR. 2014. Interactions between waves, sediment, and turbulence on a shallow estuarine mudflat. J Geophys Res Oceans. [accessed 2021 Mar 15];*119:1534–1553.* *https://doi.org/10.1002/2013JC009477*

Madsen, JD, Chambers PA, James WF, Koch EW, Westlake DF. 2001. The interaction between water movement, sediment dynamics and submersed macrophytes. Hydrobiologia [accessed 2023 Mar16]; 444:71-84. *https://doi.org/10.1023/A:1017520800568*

Morgan–King TL, Schoellhamer DH. 2013. Suspended-sediment flux and retention in a backwater tidal slough complex near the landward boundary of an estuary. Estuaries Coasts. [accessed 2021 Mar 15];36:300–318. *https://doi.org/10.1007/s12237-012-9574-z*

Morgan–King TL, Conlen AL. 2021a. Model archive summary for turbidity-derived suspended-sediment concentrations at station 11455143 Little Holland Tract North Breach, Ca. US Geological Survey. [accessed 2022 Mar 15]. *https://doi.org/10.5066/P990P1IE*

Morgan–King TL, Conlen AL. 2021b. Model archive summary for turbidity-derived suspended-sediment concentrations at station 11455167 Little Holland Tract Southeast Breach, Ca. US Geological Survey. [accessed 2022 Mar 15]. *https://doi.org/10.5066/P9F1ARTI*

Moyle PB, Herbold B, Stevens DE, Miller LW. 1992. Life history and status of Delta Smelt in the Sacramento–San Joaquin Estuary, California. Trans Am Fish Soc. [accessed 2021 Nov 10];121:67–77. *https://doi.org/10.1577/1548-8659(1992)121<0067:LHASOD>2.3.CO;2*

Nichols FH, Cloern JE, Luoma SN, Peterson DH. 1986. The modification of an estuary. Science. [accessed 2022 Jan 15];231(4738):567–573. *https://doi.org/10.1126/science.231.4738.567*

Rasmussen PP, Gray JR, Glysson GD, Ziegler AC. 2009. Guidelines and procedures for computing time-series suspended-sediment concentrations and loads from in-stream turbidity-sensor and streamflow data. In: Chapter 4 of Book 3, Applications of Hydraulics, Section C, Sediment and Erosion Techniques. US Geological Survey Techniques and Methods. 53 p. [accessed 2023 Jan 27]. Available from: *https://pubs.usgs.gov/tm/tm3c4*

Ruhl CA, Simpson MR. 2005. Computation of discharge using the index-velocity method in tidally affected areas. US Geological Survey Scientific Investigations Report 2005-5004. 31 p. [accessed 2023 Jan 26]; *https://pubs.usgs.gov/sir/2005/5004/sir20055004.pdf*

Schoellhamer DH, Wright SA. 2003. Continuous monitoring of suspended sediment in rivers by use of optical backscatterance sensors. In: Bogen J, Fergus T, Walling DE, editors. Erosion and sediment transport measurement in rivers: technological and methodological advances. IAHS Publication 283. p. 28–36.

Sommer T, Armor C, Baxter R, Breuer R, Brown L, Chotkowski M, Culberson S, Feyrer F, Gingras M, Herbold B, et al. 2007. The collapse of pelagic fishes in the upper San Francisco Estuary. El Colapso de los Peces Pelagicos en La Cabecera Del Estuario San Francisco. Fisheries. [accessed 2022 Jan 15];32(6):270–277. *https://doi.org/10.1577/1548-8446(2007)32[270:tcopfi]2.0.co;2*

Sommer T, Mejia F. 2013. A place to call home: a synthesis of Delta Smelt habitat in the Upper San Francisco Estuary. San Franc Estuary Watershed Sci. [accessed 2022 Jan 15];11(2):4. *https://doi.org/10.15447/sfews.2013v11iss2art4*

Snyder AG, Lacy JR, Stevens AW, Carlson EM. 2016. Bathymetric survey and digital elevation model of Little Holland Tract, Sacramento–San Joaquin Delta, California. US Geological Survey Open-File Report 2016–1093. [accessed 2022 Jan 15]; *https://doi.org/10.3133/ofr20161093*

Snyder AG, Stevens AW, Carlson EM, Lacy JR. 2016. Digital elevation model of Little Holland Tract, Sacramento–San Joaquin Delta, California, 2015. US Geological Survey data release. [accessed 2022 Jan 15]; *https://doi.org/10.5066/F7RX9954*

Stumpner PR, Burau JR, Forrest AL. 2021. A Lagrangian-to-Eulerian metric to identify estuarine pelagic habitats. Estuaries Coasts. [accessed 2022 Mar 15];44:1231–1249. *https://doi.org/10.1007/s12237-020-00861-7*

[USGS] US Geological Survey. 2014. Aerial Imagery. US Geological Survey (USGS) Earth Resources Observation and Science (EROS) Center. [accessed 2022 Mar 15]; *https://doi.org/10.5066/F7QN651G*

[USGS] US Geological Survey. 2016. Policy and guidance for approval of surrogate regression models for computation of time series suspended-sediment concentrations and loads. Office of Surface Water technical memorandum 2016.07. [accessed 2022 Mar 15]. Available from: *https://water.usgs.gov/admin/memo/QW/qw2016.10.pdf*

[USGS] US Geological Survey, 2020. National Water Information System: US Geological Survey web interface. [accessed 2020 August 15]. Available from: *https://nwis.waterdata.usgs.gov/nwis*

Work PA, Downing–Kunz M, Drexler JZ. 2021. Trapping of suspended sediment by submerged aquatic vegetation in a tidal freshwater region: field observations and long-term trends. Estuaries Coasts. [accessed 2022 Jan 15];44:734–749. *https://doi.org/10.1007/s12237-020-00799-w*

Wright SA, Schoellhamer DH. 2004. Trends in the sediment yield of the Sacramento River, California, 1957–2001. San Franc Estuary Watershed Sci [accessed 2022 Jan 15];2:1–14. *https://doi.org/10.15447/sfews.2004v2iss2art2*

Wright SA, Schoellhamer DH. 2005. Estimating sediment budgets at the interface between rivers and estuaries with application to the Sacramento–San Joaquin River Delta. Water Resour Res. [accessed 2022 Jan 15]; 41:W09428. *https://doi.org/10.1029/2004WR003753*